37. CYCLIC SEDIMENTATION ALONG THE CONTINENTAL MARGIN OF NORTHWEST AFRICA

Walter E. Dean,[1] James V. Gardner,[2] Lubomir F. Jansa,[3] Pavel Čepek,[4] and Eugen Seibold[5]

INTRODUCTION

One of the most striking characteristics of the sediments cored along the west African continental margin on Leg 41 is their cyclicity. Three main types of cycles are recognized: (1) cycles representing fluctuations in supply of terrigenous components due to turbidity currents, (2) diagenetic cycles due to fluctuations in *p*H and Eh (redox) conditions in the sediments and possibly bottom waters, dissolution and reprecipitation of $CaCO_3$, and dissolution and reprecipitation of SiO_2; and (3) pelagic cycles of $CaCO_3$ and clay due to fluctuations in $CaCO_3$ dissolution and(or) noncarbonate dilution.

In the following discussions, we will use the term "period" to describe the number of years required, on the average, to deposit a cycle. Periods are calculated by measuring the number of cycles in a sequence measured over tens of meters falling between biostratigraphic age boundaries. Time was determined by the age difference of these biostratigraphic boundaries, thus a cycle period was established. We realize that measured thicknesses are compacted thicknesses and that some have undergone dissolution and(or) diagenetic alterations in addition to compaction. However, we feel that because of inherent errors in absolute age calibrations, judgments about the amount of volume reduction would be senseless at this time. Our calculations of periods should be considered in light of the above restrictions.

DESCRIPTION OF TURBIDITE CYCLES

The most common cyclic sediments cored on Leg 41 are turbidites. Turbidites are particularly well developed in the lower Miocene through Upper Cretaceous sediments at Site 368 on the Cape Verde Rise, but are also common at Site 367 in the Cape Verde Basin off Senegal and at Site 370 in a deep basin off Morocco (Figure 1). Most of the turbidites are fine grained and consist mainly of cycles of clay, with periods on the order to 10,000 yr.

Cycles of light green and dark green claystone in Core 22, Section 3, from Site 368, illustrated in Figure 2a, are typical of the simple couplets composing the section from lower Miocene through upper Eocene.

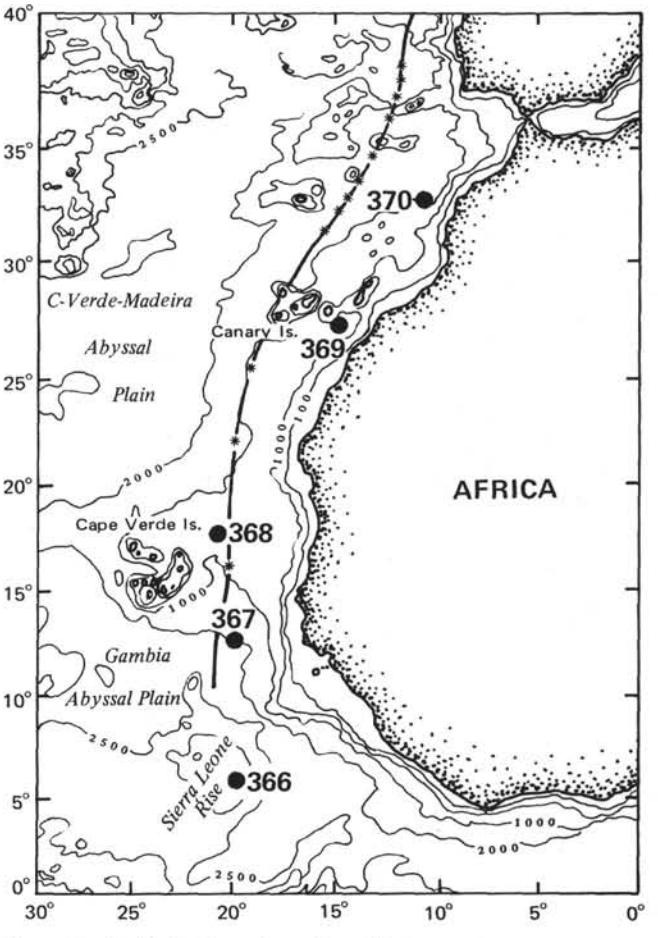

Figure 1. *Drill site locations, Leg 41.*

The contact between a dark claystone and an underlying lighter claystone is usually a sharp break in color, whereas the upper contact is usually gradational. Some boundaries are obscured by bioturbation. These cycles average about 12 couplets per 1.5 meters, giving a period of about 12,500 yr, based on an accumulation rate of 1 cm/10^3 yr. Claystone couplets in middle and lower Eocene turbidites are complicated by addition of chert or porcellanite beginning in Core 23, Section 2 (Figure 2b). The chert or porcellanite commonly occurs at the base of the darker member of well-defined claystone couplets, suggesting that a decrease in depositional porosity upward through a couplet may have resulted in a tendency for SiO_2 precipitation at the base. The turbidites in the lower Eocene (from about Core 33, 446 m to Core 44, 620 m) become darker, harder, and siltier. Chert or porcellanite do not occur below Core 44, Section 3, although well-developed

[1]U.S. Geological Survey, Denver, Colorado.
[2]U.S. Geological Survey, Menlo Park, California.
[3]Geological Survey of Canada, Dartmouth, Nova Scotia.
[4]Bundesanstalt fur Geowissenschaften und Rohstoffe, Hannover, Federal Republic of Germany.
[5]Geological Institute, Kiel University, Kiel, Federal Republic of Germany.

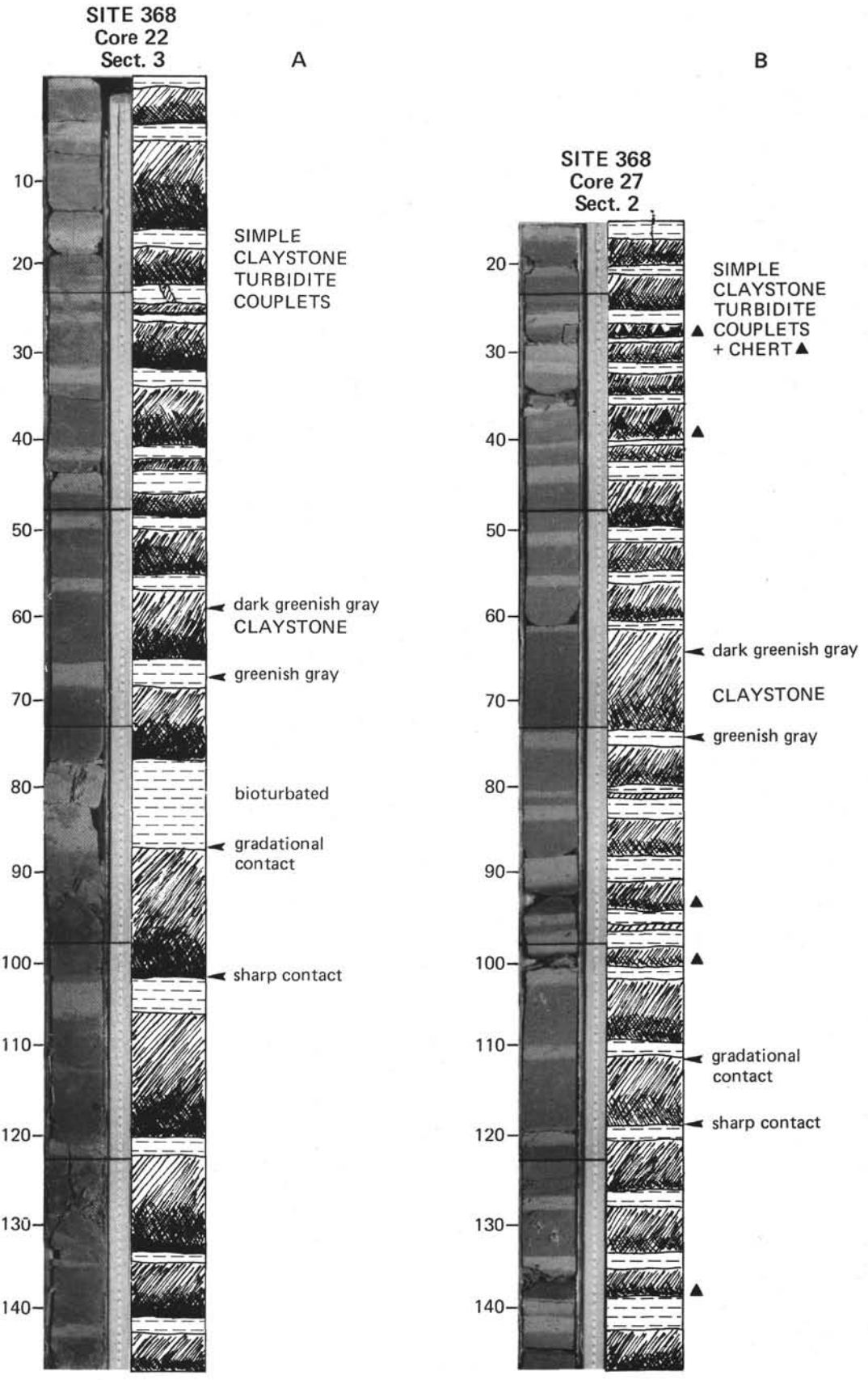

Figure 2. *Turbidite cycles, Site 368. (A) Simple claystone couplets; (B) Simple claystone couplets + chert.*

turbidites continue at least through Core 47, 665 meters. (Cores 48 and 49 had no recovery.) Turbidites below the chert at Site 368 consist of olive black and dark greenish-gray claystone couplets.

Siderite?-cemented sandstone or siltstone laminae also commonly occur at the bases of the darker claystone layers (Figure 3a). More than 50% of the section in Core 46, Section 3, is carbonate-cemented siltstone. The bases of many siltstone and sandstone laminae display what appear to be load casts. These coarser layers are argillaceous, with quartz as the predominant coarse component. The quartz grains are subrounded and often polycyclic (rounded overgrowths on rounded quartz nuclei). In addition to quartz, minor plagioclase, microcline, heavy minerals, and mica are characteristic components of the coarse clastics. The composition of the coarse clastics clearly indicates that this material was derived from the African continent and not from local volcanic sources. The thin sandstone or siltstone layers grade rapidly into the overlying claystone layers. The gradation is one of grain size and not of color, because both sandstone and claystone layers are the same approximate color (usually olive). The olive claystone layer is usually structureless, with occasional "floating" quartz grains. The olive claystone layer then grades by color change into the overlying lighter green claystone. The upper light-colored claystone layers contain fine, wispy laminae and are commonly bioturbated. The lighter green claystone layer, like the underlying darker claystone layer, usually contains "floating" quartz silt grains, although they are not as abundant. The silt grains are often concentrated in the wispy laminae and in burrows.

Turbidites from Cores 23 through 47 at Site 368 average about 6 to 8 cm/cycle and have average periods of about 6000 to 8000 yr, based on an average accumulation rate of 1 cm/10^3 yr. However, we must point out that biostratigraphic control at this site is poor throughout most of the turbidite sections. The rate of 1 cm/10^3 yr is certainly a minimum value, and the actual accumulation rate of the turbidites was probably considerably faster.

At Site 367 in the Cape Verde Basin, silt turbidites are superimposed on cycles of green clay and black shale of late Aptian to early Turonian age (Figure 3b). The silt turbidites occur in Cores 19 through 23 (644.5 to 787 m), but are particularly well defined in Cores 21 and 22, where they average about 20 cm per cycle. Average rates of accumulation for this section are around 2 cm/10^3 yr, giving an average period of about 10,000 yr per turbidite cycle.

At Site 370, in a deep basin off Morocco, turbidites compose most of the 1200-meter section that was recovered. The turbidites at Site 370 are much coarser than turbidites at either Site 367 or Site 368, and are often conglomeratic. The coarser components are usually terrigenous quartz with glauconite mudstone clasts, fish debris, and shelf carbonate clasts, and some dolomitic oolites. Concentrations of heavy minerals within the turbidites suggest that the material may have been considerably reworked. Slump deposits are common throughout the section. The entire section at Site 370, with the exception of the Pleistocene, is hemipelagic, and was probably deposited in a submarine fan (see Lithologic Description, Site 370 chapter, and Lithologic Synthesis for more detailed descriptions of these sediments). These turbidites do not seem to have a dominant periodicity.

DESCRIPTION OF DIAGENETIC CYCLES

Cycles of Redox Conditions

Most of the redox cycles are defined on the basis of color and largely reflect the organic content of the sediments. These cycles are best developed at Site 367 in the Cape Verde Basin, where most of the section is characterized by variations in content of organic matter. In the Eocene (Core 8, 302.5 to 312 m), these cycles occur as alternating greenish-gray and black clays (Figure 4a). The lower contact of a black clay layer is always sharp; the upper contact is usually sharp, but may be gradational. Bioturbation is common in greenish-gray clay, but rare in black clay. On the basis of examinations of smear slides, no differences between the green and black clays are apparent, except for content of organic matter; black clays have organic-carbon concentrations as high as 4%, whereas organic-carbon concentrations in the green clays are commonly between 0.1% and 0.3%. Accumulation rates for this part of the section are fairly well established and indicate an average of about 0.6 cm/10^3 yr, which gives a period of about 50,000 yr/cycle.

Alternating green and black clays occur in Cores 9 through 14 (331 to 388 m), but black clay interbeds are less frequent. Radiolaria and diatoms are generally absent in green clay but are present yet rare in black clay. Fish debris, quartz, and occasionally glauconite are found only within black-clay layers. Green clay is generally barren and bioturbated, and contains common to abundant clinoptilolite. This part of the section is complicated by bedded chert and porcellanite intercalated with the clay. These cycles may be equivalent to cycles of green and olive-gray clay of early to middle Eocene age observed at Site 140 (Cores 3 and 4) on DSDP Leg 14 (Hays, Pimm, et al., 1972).

Pulsing of organic matter is also suggested by the late Aptian to Turonian cycles of green and black shale in Cores 17 through 23 (616-787 m, Figure 4b). The organic-carbon content of black shale is commonly around 5% and may be as high as 28% (Core 18, Section 2, 34 cm). In Cores 18 through 23, black shale containing plant fragments, palynomorphs, and fish debris is the dominant lithology. Cycles of silt turbidites (discussed above) are superimposed on cycles of green and black shale in Cores 21 through 23 (Figure 3b). These cycles are probably lithic equivalents of the Cenomanian cycles of carbonaceous black mud and greenish-gray, dolomitic-silty clay cored at Site 138 (Core 6, Section 3) on DSDP Leg 14 (Hays, Pimm, et al., 1972).

Cyclic alternations of redox conditions during which the sediments occasionally became intermittently oxidized are suggested by alternating reddish-brown

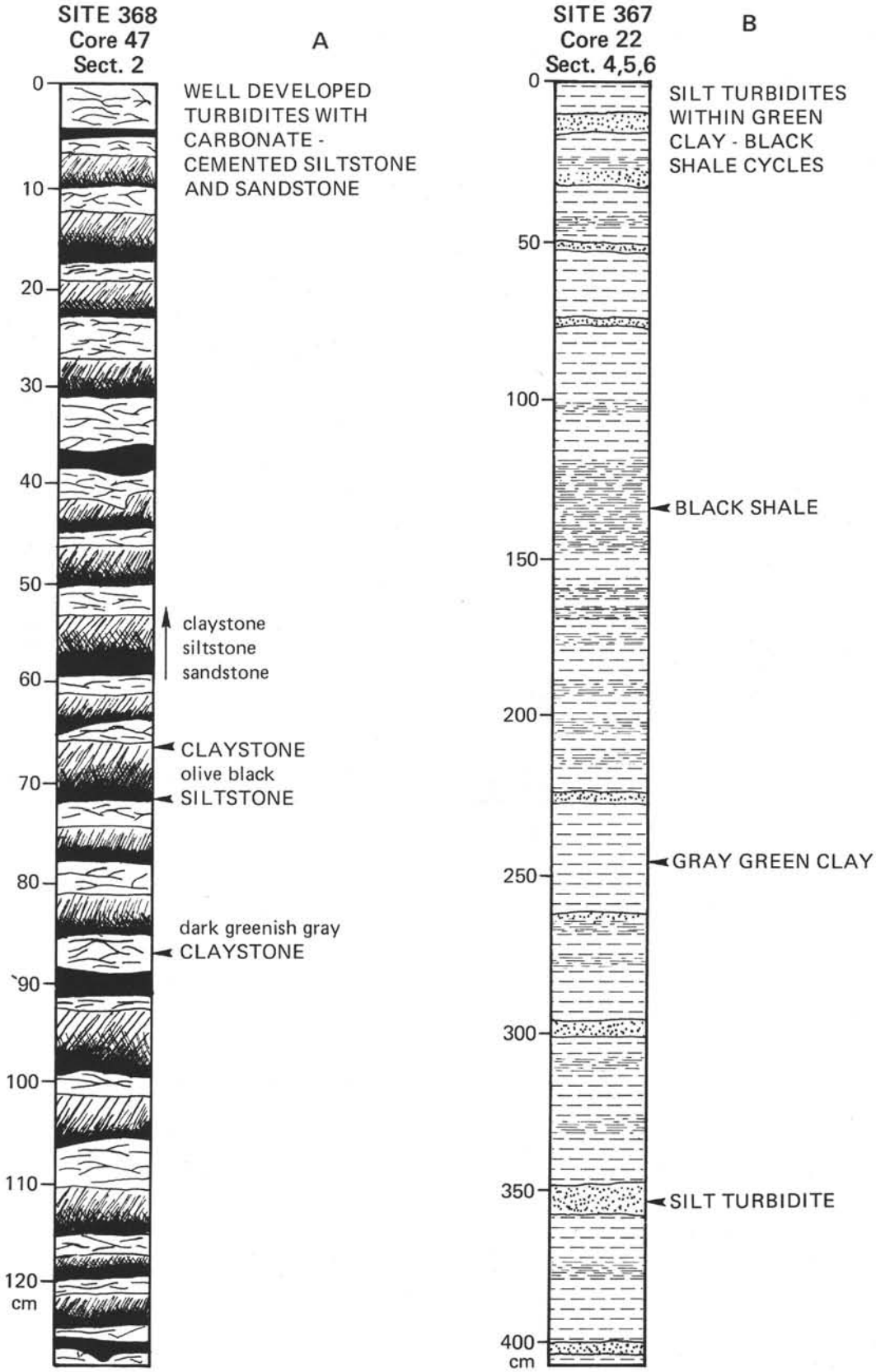

Figure 3. *Turbidite cycles, Sites 367 and 368. (A) Turbidites with carbonate-cemented siltstone and sandstone, Site 368; (B) Silt turbidite within green and black clay cycles, Site 367.*

and blue-green silty clay in Cores 15 and 16 (Figure 4c). Biostratigraphic control in this part of the section at Site 367 is poor, but accumulation rates can be estimated at about 0.6 to 0.8 cm/10^3 yr. These

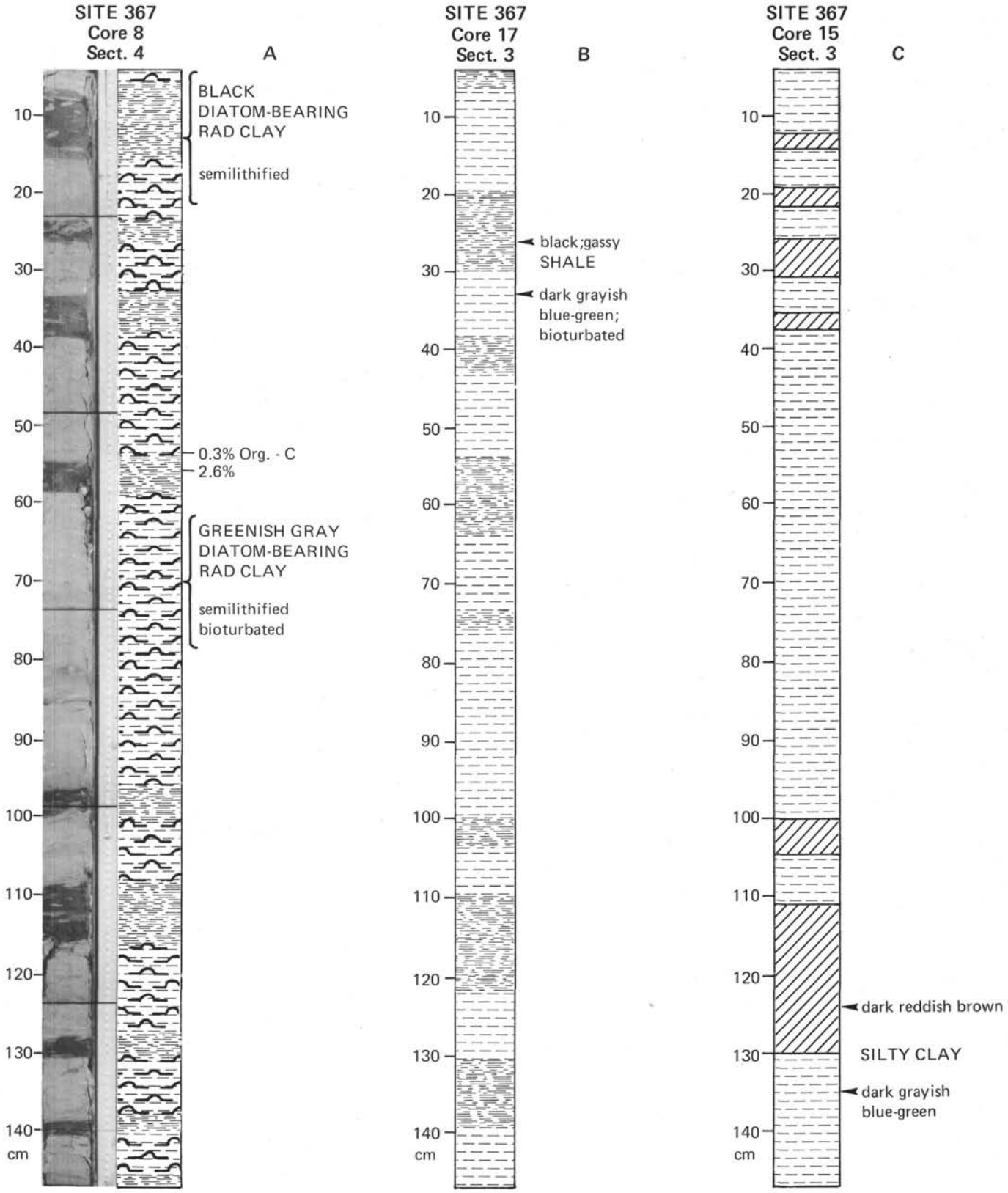

Figure 4. *Redox cycles, Site 368. (A) Black and green rad clay cycles; (B) green and black shale cycles; (C) green and red silty clay cycles.*

sedimentation rates yield cycle periods on the order of 50,000 yr, or about the same as the periods of Eocene cycles of green and black clay, and Middle to Late Cretaceous cycles of green and black shale. Organic carbon contents of both the red and green silty clays (ca. 0.1%) are lower than those of the Eocene and

Cretaceous green clays. Examination of smear slides of both red and green silty clays suggests greater input of terrigenous material than is found in either overlying Eocene clay or underlying Cretaceous shale. Although clay is the dominant component, silt-size quartz is common to abundant; and feldspars, heavy minerals, and fish debris are persistent but rare. These red and green clay cycles at Site 367 are probably equivalent to the red-brown, blue-green shale cycles of the Upper Cretaceous to Paleocene(?) at Site 368 (Cores 5 through 52, 702.5-731 m).

Another period of diminished input of organic material in the Cape Verde Basin, which resulted in variations in oxidizing and reducing conditions in the sediments, is represented by the interbedded red and green claystones in Core 24. These claystones are sandwiched between cycles of black and green shale in Cores 7 through 23 (Figure 4b) and organic-rich cycles of marlstone and light-gray limestone in Cores 25 through 32 (Figure 5).

The cycles of light gray limestone and dark olive marlstone of Barremian through Tithonian age at Site 367 (Cores 25 to 32, 891.5-1089 m, Figure 5) represent a striking contrast to the overlying clay cycles, but are still interpreted as a manifestation of pulsing organic input. The couplets in Core 26, where the limestone-marlstone cycles are particularly well developed, have an average period of about 37,000 yr, using an accumulation rate of 0.6 cm/10^3 yr.

Note in Figure 5 that the carbonate content varies from less than 50% in marlstone to more than 90% in limestone.[6] Organic carbon content varies from greater than 1% in marlstone to less than 0.1% in limestone. Shipboard organic-carbon analyses show that the marlstone may contain as much as 4% organic carbon, and a "coal" lens in Core 26, Section 4, 31 cm has an organic carbon content of 33%. Bioturbation is restricted to gray limestone, and marlstone is characterized by an abundance of fine, delicate laminations and pyrite lenses.

We interpret the Eocene cycles of green clay black clay to represent pulses of high-organic terrigenous material (black clay) superimposed on normal pelagic-clay sedimentation. The above-average accumulation rate (0.6 cm/10^3 yr) supports this contention. Cyclic variations in supply of this terrigenous material may, in turn, be related to climatic cycles during the Eocene. This cyclicity apparently continues through the Holocene at Site 367, as evidenced by cyclic interbeds of nanno marl and silty clay in Cores 1 to 7 (0 to 302.5 m). Unfortunately, however, severe drilling disturbance obliterated almost all of these cycles.

The presence of black mud or shale in the deep sea is often interpreted as indicating stagnant bottom conditions (e.g., Nesteroff, 1973; Bolli, Ryan, et al., 1975). This may be a plausible explanation for extensive black muds and shales such as the Albian and Aptian black shales of the Atlantic, and for their presence in restricted basins such as the Black and Mediterranean seas. However, we do not think it applies to this region off northeast Africa. The cyclic alternation of pelagic clay and muds, rich in organic and terrigenous clastic materials adjacent to a continent known for its delicate balance between arid and humid-tropical climatic conditions, suggests that the mechanism may be climatically induced pulses of terrigenous material. The bottom waters were probably well oxygenated during intervals of pelagic-clay deposits, because the green clays are intensely bioturbated. Although several tenths of a percent of organic carbon in the green clay is an order of magnitude lower than concentrations of organic carbon in the black clay, it is still an order of magnitude higher than the organic-carbon concentration in most open-ocean pelagic clay (see the geochemistry section of Site Reports Initial Reports from any of the mid-ocean legs of DSDP). During intervals of high-organic influx, reducing conditions which resulted from decay of organic matter probably extended upward at least a short distance into the bottom waters, as suggested by the apparent lack of bioturbation in the black clays. Diminished bottom-water circulation may have helped to maintain low oxygen conditions above the sediment-water interface and may have controlled the thickness of deoxygenated bottom water. Bottom-water stagnation is not a necessary cause for creation of reducing conditions within the sediments or even within water just above the sediment-water interface.

We feel that the cycles of red and green silty clay and claystone from Site 367 may be the result of subtle differences in climatically derived organic input. These intervals probably represent periods of generally reduced input of organic matter, sandwiched between periods of higher input of organic matter represented by cycles of green and black shale of late Aptian to early Turonian age and cycles of green black clay of Eocene age.

To summarize the stratigraphy of the cycles at Site 367, pulsing of organic matter, assumed to have been derived largely from the African continent, began in the Late Jurassic and continued through at least the Eocene. We found the oldest cycles in the light gray limestone, olive-marlstone cycles of the Oxfordian-Kimmeridgian to upper Aptian-lower Albian section, followed by green and black clay cycles of the upper Aptian-lower Albian to lower Turonian and Eocene sediments. Intervals of lower organic input, permitting oxidizing conditions in the sediments, are represented by green and red claystone cycles in the Upper Cretaceous, and by red and green silty clay cycles of the Upper Cretaceous-lower Tertiary.

Cycles of Dissolution and Reprecipitation of $CaCO_3$

Another possible example of diagenetic cycles, also found in the Cape Verde Basin (Site 367), is illustrated by alternating light green and red nodular limestone of Late Jurassic age (Figure 6). The red limestone is argillaceous, with common nannofossils, wavy laminations, and burrows. The interbedded pale green

[6]Because photography, lithologic description, and sampling for carbonate and organic carbon were done on different halves of the core, slight differences in depth reference may occur. Consequently, the low-carbonate portions of the analysis curve in Figure 5 do not always match the low-carbonate portions of the lithologic column.

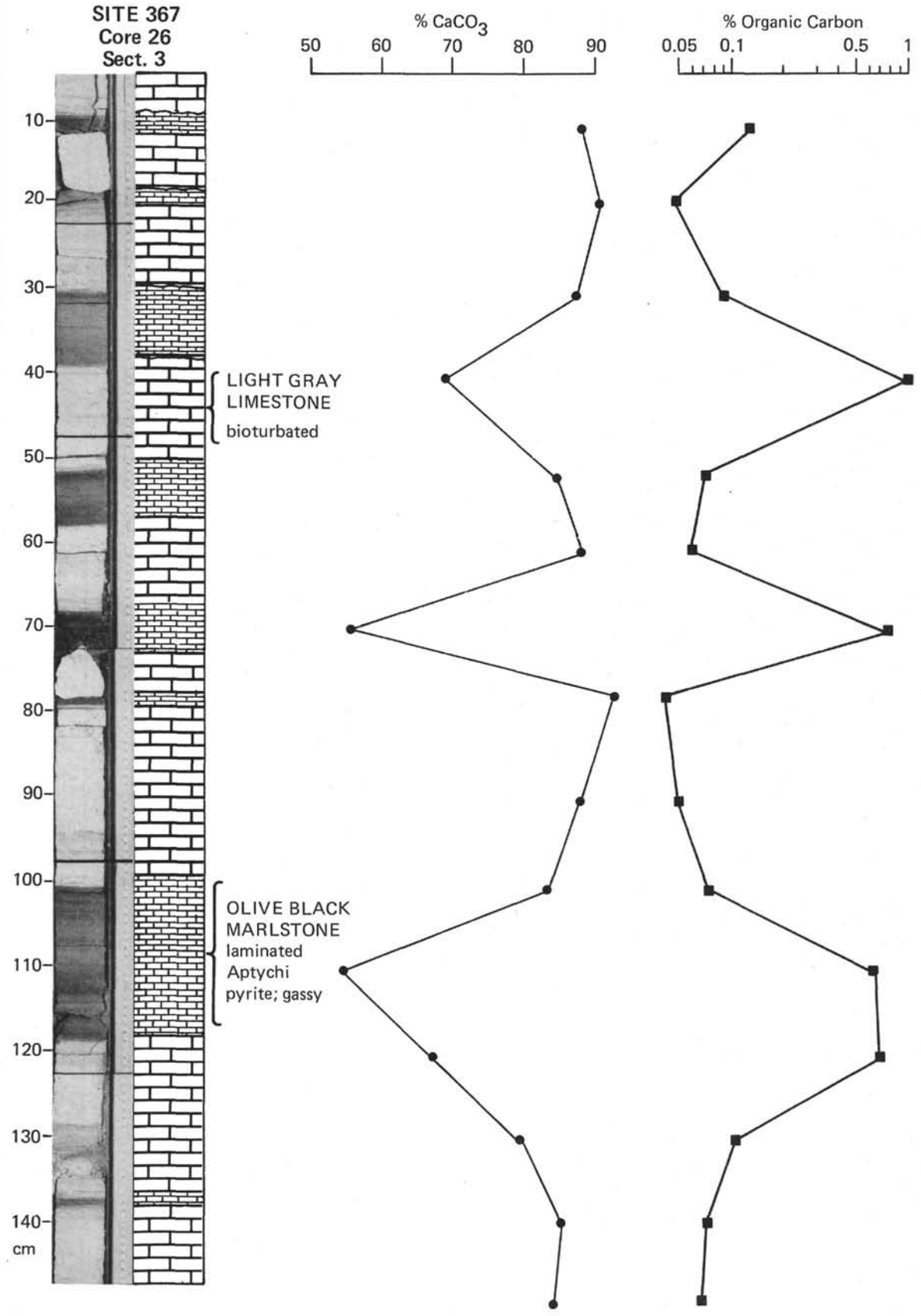

Figure 5. *Cycles of light gray limestone and organic-rich olive marlstone, Site 367.*

and gray limestone usually consists of boudinage structures or coalescing nodules giving the beds wavy, uneven upper and lower contacts. Both red and green limestones are very well cemented, and stylolites are

Figure 6. *Core photograph of light green and red nodular limestone, Site 367, Core 34, Section 4.*

common. These units are virtually identical to red and white nodular limestones cored at Sites 99, 100, and 105 in the western Atlantic (Hollister, Ewing, et al., 1972). The Jurassic limestones at all four sites (Sites 99, 100, 105, and 367) are considered to be equivalent to the Ammonitico Rosso facies of the classic Jurassic Tethyan sections of the Mediterranean (Bernoulli, 1972; Bernoulli and Jenkyns, 1974; Jansa, this volume).

Cyclic alternation of red and light gray or light greenish-gray limestone is certainly the result of cyclic diagenetic conditions. Because of the post-Jurassic history at Site 367 and because of fluctuating input of organic material elsewhere, it would be tempting to relate the red and green coloration of the limestones to fluctuating diagenetic redox conditions within the sediments, in much the same way that we have attempted to relate the younger red and green cycles of Sites 367 and 368 to diagenetic redox fluctuations (see previous discussion). Two other models have been suggested, both involving diagenetic fluctuations in dissolution of aragonite (largely from ammonites, as evidenced by ammonite molds) and reprecipitation of the $CaCO_3$ as light colored calcite nodules within a red, argillaceous lime mud matrix (Jenkyns, 1974; Bosellini and Winterer, 1975). The Bosellini and Winterer (1975) model suggests cyclic variations in the Jurassic positions of the aragonite and calcite lysoclines and compensation depths. They suggest that all four levels were close together and shallow (less than 3000 m) during the Late Jurassic. Cyclic fluctuations in these levels would produce cyclic fluctuations in rate of dissolution of aragonite, which could be used to explain the cyclic interbeds of red and light gray limestones of the Ammonitico Rosso. A third model, proposed by Jenkyns (1974), also uses early diagenetic dissolution of aragonite and fine-grained calcite as the origin of alternating nodule-rich and clay-rich layers in the Ammonitico Rosso. However, in Jenkyns' model, the cyclicity is the result of periodic build-up of calcite supersaturation relative to the position of the sediment-water interface. According to this model, most dissolution of aragonite takes place at the sediment-water interface. This suggestion is supported by evidence that Holocene calcite nodules have formed on the floor of the Mediterranean (Müller and Fabricius, 1974). Once interstitial waters become supersaturated with respect to calcite, formation of calcite nodules begins, probably by precipitation around a nucleus. Development of nodules slows as sedimentation moves the sediment-water interface upward away from the zone of active nodule growth. Once covered, the nodule eventually stops growing as $CaCO_3$ in interstitial water is depleted. With time, dissolution of aragonite again builds up the degree of supersaturation with respect to calcite to the point of formation of a new layer of calcite nodules. Spacing of the nodular zones is thus the result of rate of accumulation (i.e., rate of upward migration of the sediment-water interface), rate of aragonite dissolution, and rate of $CaCO_3$ depletion by nodule growth within the sediments. Our data do not favor any one explanation over the other two.

Cycles of Dissolution and Reprecipitation of SiO_2

It is not our intention in this section to tackle the complex and controversial problem of origin of chert and porcellanite. A discussion of this problem, as it relates to the occurrence of chert and porcellanite in Leg 41 cores, is presented elsewhere (see von Rad, this volume). However, we are impressed with the relationships of silica diagenesis to cyclic sedimentation in Leg 41 cores, sometimes superimposed on other cycles and sometimes apparently forming separate cycles.

The extent of development of lower and middle Eocene chert and porcellanite is particularly impressive. Chert and porcellanite at Sites 368 and 370 occur as nodules and beds within thick turbidite sections. As discussed above, chert and porcellanite usually occur within lower members of turbidite couplets, suggesting that perhaps primary porosity exerted some control on silica diagenesis. Bedded chert and porcellanite at Site 367 occur within Eocene cycles of zeolitic green and black clay. Chert also occurs within limestone of the Lower Cretaceous cycles of light gray limestone olive-black marlstone at Site 367. Nodules, thin stringers, and layers of chert and porcellanite are common in Jurassic red and gray

nodular limestone at Site 367. Here, silica replacement usually occurs just above a red marlstone or argillaceous layer.

Well-developed cycles of SiO_2 and $CaCO_3$ are characteristic of lower and middle Eocene sediments at Site 366 on the Sierra Leone Rise (Cores 17 to 37, 480-680 m). The basic lithologies of these cycles are light greenish-gray chalk alternating with light gray siliceous limestone, porcellanite, or chert. A typical cycle consists of about 5 cm of nanno chalk overlying about 10 cm of silicified limestone or porcellanite. Chert nodules occur in the bottom 5 cm of some siliceous limestone and porcellanite. The siliceous limestone is apparently the result of cementation of light gray nanno chalk with both SiO_2 and $CaCO_3$, as suggested by common siliceous halos adjacent to porcellanite beds. Several excellent samples of the transition from porcellanite into siliceous limestone into unlithified chalk occur in Hole 366, Core 23, Sections 1 and 2. The silica cycles are, therefore, secondary, resulting from selective silicification of the light gray chalk, probably in response to greater primary porosity.

The primary unlithified cycles are alternating light-green and light-gray chalk, which we interpret as dissolution cycles. Green chalk contains more clay than does light gray chalk, and consequently has a lower content of $CaCO_3$ (ca. 80% $CaCO_3$ for green chalk; ca. 90% $CaCO_3$ for gray chalk). Also, gray chalk contains abundant, well-preserved nannofossils, coccoliths being much more abundant than discoasters. However, in green chalk, nannofossils are much less abundant and are dominated by more dissolution-resistant discoasters. We interpret the higher clay content of green chalk to be the result of carbonate dissolution rather than clay dilution (discussed in greater detail in the next section). Lithification at Site 366 was first detected in Core 17. Here, light gray chalk was cemented by both SiO_2 and $CaCO_3$. Both degree of cementation and clay content increase with depth; and, by Core 24 (547 m), most light-gray chalk is completely cemented. By Core 29 (594 m), the cycles are alternations of siliceous and argillaceous limestone. Both lithologies contain abundant euhedral to subhedral calcite cement, and nannofossils are almost completely recrystallized.

DESCRIPTION OF CARBONATE-CLAY CYCLES

Cycles of high $CaCO_3$ and low carbonate or noncarbonate sediments with periods on the order of tens of thousands of years occur in the lower Pliocene to lower Miocene carbonate section on the Cape Verde Rise (Site 368, Core 5, 122 m, through Core 16, 266 m), but they are best developed and much more continuous in Eocene through middle Miocene sediments at Site 366 on the Sierra Leone Rise. We use the term "clay" below for fine-grained sediment with little or no biogenic component.

Water depth at Site 368 is only 3367 meters, well above the present calcite compensation depth (CCD), and we, therefore, anticipated a much thicker carbonate section than we actually cored. However, this site has apparently been a topographic rise only since the Miocene (see Site 368 chapter, this volume); the pre-Miocene section consists mainly of well-developed turbidite cycles, indicating a pulsed input of terrigenous clastic material. Carbonate accumulation began in early Miocene (Core 16, 266 m) as cycles of nanno marl and clay; it continues upward with decreasing clay content, until finally, in early Pliocene (Core 5), cycles of nanno-ooze and marl occur with a $CaCO_3$ variation from about 80% in ooze to about 60% in marl (Figure 7b). These Pliocene cycles are distinct in color with sharp lower contacts and gradational upper contacts. The sedimentation and tectonic histories at Site 368 would suggest that the carbonate-clay cycles are the manifestation of pulsed input of terrigenous material — either from fine-grained suspensions within tails of bypassing turbidity currents, as in the lower Tertiary, or from fluctuations in pelagic clay superimposed on a rain of pelagic carbonate debris. Overall, carbonate should have become increasingly better preserved (i.e., less dissolution occurred), as the site was uplifted above the CCD. Increased preservation of carbonate is indicated by increasing abundance and degree of preservation of both forams and nannos (Figure 8 and Diester-Haass, this volume). The increasing content of $CaCO_3$ in the younger nanno oozes is, therefore, the combined result of increasing

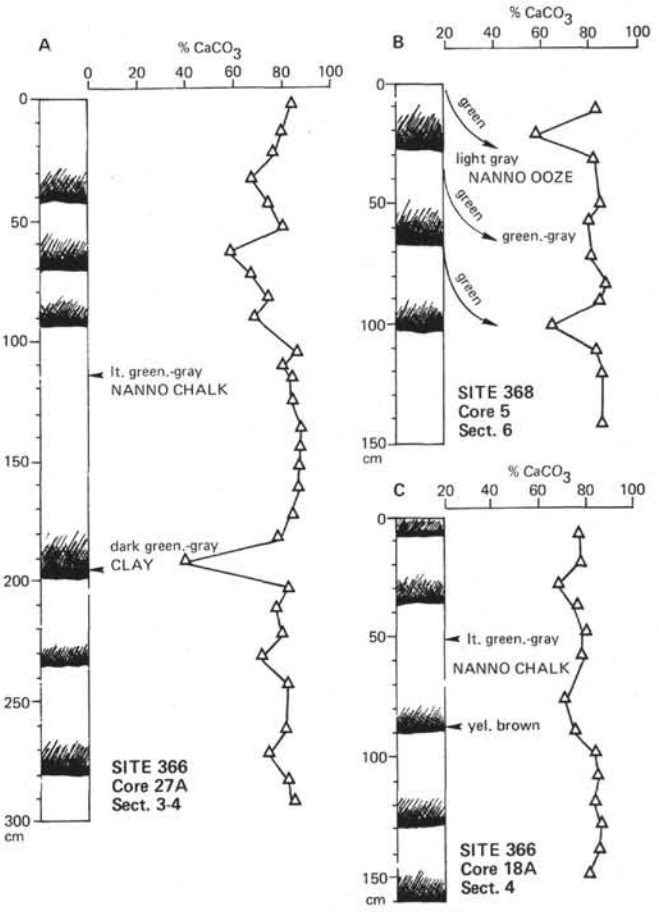

Figure 7. *Carbonate-clay cycles, Sites 366 and 368. (A) Nanno chalk and marl cycles, Hole 366A; (B) nanno ooze cycles, Site 368; (C) nanno chalk cycles, Hole 366A.*

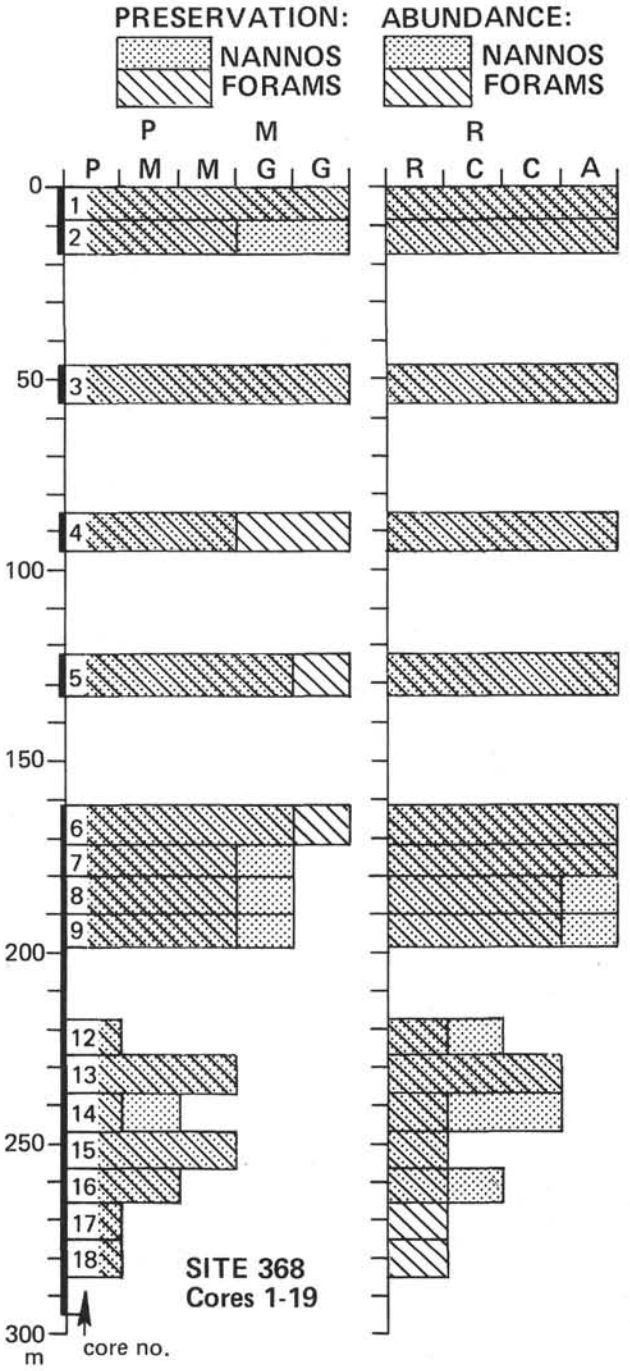

Figure 8. *Histograms of relative preservation and abundance of calcareous plankton, Site 368, Cores 1-19. P = poor, M = moderate, G = good; R = rare, C = common, A = abundant.*

carbonate preservation and decreasing dilution by terrigenous clastics.

Another possibility is that the clay component in $CaCO_3$-clay cycles at Site 368 is not the result of pulsed clastic dilution, but rather is the residue resulting from cyclic variations in dissolution of $CaCO_3$ once the site became a topographic rise. This would presuppose that either turbidity current activity, so prevalent in the entire pre-middle Miocene section, stopped, or that the slight topographic difference (several hundred meters) between the newly-created rise and the surrounding basin was sufficient to isolate the site from turbidity currents.

The situation at Site 366 is a little different. The site is in a water depth of 2860 meters on the eastern edge of the Sierra Leone Rise. The Sierra Leone Rise appears to have been a prominent topographic rise throughout most of its history. At present, the top of the rise is 1500 to 2500 meters above the surrounding abyssal plain and is bounded on all sides by relatively steep slopes. We continuously cored an uninterrupted 850-meter pelagic carbonate record of the entire Cenozoic at Site 366. The sediments are nanno ooze, grading downward into chalk and marl, and then into limestone and marlstone. The middle and lower Eocene sediments contain abundant chert and porcellanite. Most chalk, marl, and limestone show cyclic alternations of clay-rich and clay-poor calcareous beds having average cycle thicknesses between 40 and 70 cm. The average accumulation rate, based on excellent biostratigraphic control, is relatively constant at 1.4 cm/10^3 yr (Figure 9), which yields cycle periods on the order of 30,000 to 50,000 yr. Contents of $CaCO_3$ are generally around 80% in clay-poor portions of the cycles and 60% to 70% in clay-rich portions, although they may vary from greater than 90% to less than 20%. The average of 121 $CaCO_3$ analyses for the section above the initiation of silica diagenesis (Core 16, 480 m) is 74%.

Well-developed cycles of $CaCO_3$ and clay at Site 366 were first noticed at the top of the middle Miocene section (Core 15A, 136 m) where they occur as alternating nanno ooze and nanno marl. By 158 meters depth (Core 18A), the sediment is well indurated, and the cycles are of chalk and marl (Figure 7c). Well-developed chalk-marl and chalk-clay cycles continue

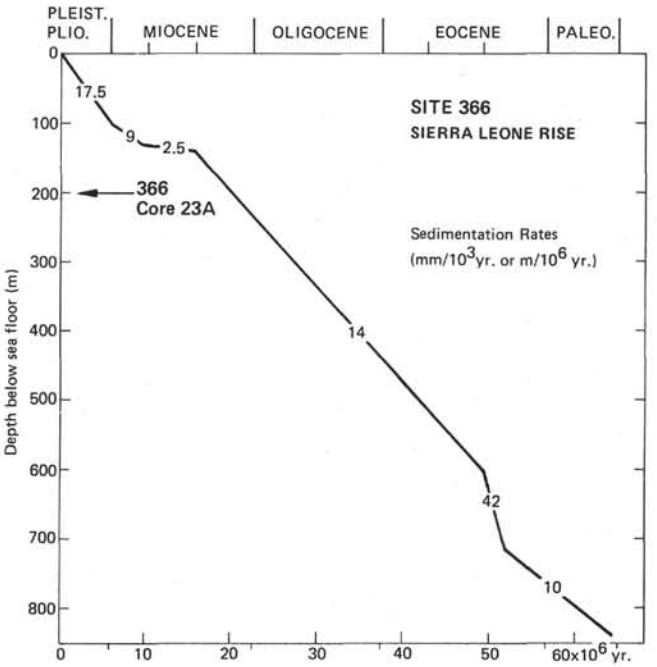

Figure 9. *Biostratigraphix accumulation rate curve, Site 366.*

from Core 16A through Core 16 (Hole 366, middle Eocene, 489 m).

At the time the shipboard descriptions were made, the cycles were recognized mainly on the basis of sediment color and consistency, with smear-slide observations and $CaCO_3$ determinations to further describe lithologies involved. Chalks were commonly light greenish gray, grading gradually downward into greenish-gray or dark greenish-gray marl or clay.[7] The color change from greenish-gray marl to the underlying light greenish-gray chalk was usually abrupt. These color differences suggest that each cycle is assymetrical, with a sharp lower contact but a gradual change upward into lighter colored chalk. Several sections through well-developed cycles were later sampled at 10-cm intervals to further define the cycles in terms of $CaCO_3$ content. The iron in the sediments oxidized in the few months between the time the cores were collected and the time they were sampled on shore, and most of the green coloration is now gone. Analyses of the post-cruise samples showed that $CaCO_3$ differences were greatest where color differences had been most pronounced, ranging from greater than 80% to less than 10%. Where fresh color differences had been more subtle, $CaCO_3$ differences are slight or nonexistent, and oxidation has erased color differences (e.g., Figure 7c). Some of the fresh color boundaries were, therefore, indicating cyclic variations in sediment composition that were not always the result of relative $CaCO_3$ content. All interbedded lithologies are intensely bioturbated, although the burrows were easier to recognize in the darker, clay-rich members of cycles where lighter sediment has been bioturbated into darker (see Harrington, this volume).

Table 1 shows some typical average cycle thicknesses for the chalk-marl cycles of late Eocene to middle Miocene age at Site 366. The cycle thicknesses yield periods ranging from 29,000 to 50,000 yr, using an average accumulation rate of 1.4 cm/10^3 yr (Figure 9).

The cycles of $CaCO_3$ and clay in the middle and lower Eocene portions of the section are complicated by the addition of chert or porcellanite. As discussed in the previous section, we believe that portions of the cycles highest in $CaCO_3$ were preferentially cemented by both SiO_2 and $CaCO_3$. The cycles beginning in Core 17 (480 m) consist of interbedded nanno chalk or marl and siliceous limestone (Figure 10), and finally (Core 29, 594 m) of interbedded siliceous limestone and argillaceous limestone or marlstone. Well-defined siliceous-argillaceous limestone cycles end at about Core 38 (680 m), but hints of cyclicity continue through the Paleocene section (ca. Core 48, 775 m).

Some typical, average-cycle thicknesses for the Eocene siliceous portions of the section are given in Table 1. Somewhere around the lower-middle Eocene boundary (ca. Core 29, 594 m), the average accumulation rate decreased from 4.2 cm/10^3 yr to 1.4 cm/10^3 yr (Figure 9). This horizon roughly corresponds to the change from cycles of siliceous and argillaceous limestone to cycles of nanno chalk or marl and siliceous limestone. These accumulation rates, applied to the above-average cycle thicknesses, yield periods of about 14,000 to 21,000 yr in Cores 19 through 28, and 7000 to 14,000 yr for Cores 29 through 36.

TABLE 1
Typical Average Cycle Thicknesses for Chalk-Marl Cycles of Eocene to Miocene Age and Chalk-Siliceous Limestone Cycles of Eocene Age, Site 366

Core	Thickness of Cycle (cm)
18A	40
23A	65
27A	63
34A	70
37A	68
38A	46
39A	50
5	60
10	47
19-24	26-30
25-28	20
29	33
21	35
32-33	30
35	38
36	58

A section at Site 366 showing several well-developed lower Miocene chalk-marl cycles (Core 23A, Sections 1 and 2) was sampled at 10-cm intervals, and the samples were split for analyses of $CaCO_3$, organic carbon, clay mineralogy, and quantitative and qualitative variations in nannofossil content. A 1-meter section through two of these cycles showing extreme variation in $CaCO_3$ content was sampled at 5-cm intervals to define the cycles in greater detail ($CaCO_3$ and organic carbon analyses by F.C. Kögler, Kiel University).

Figure 11 shows that there are no qualitative differences in carbonate-free clay mineralogy between high- and low-$CaCO_3$ portions of the cycles, with quartz and kaolinite as the dominant crystalline materials and high but variable amounts of X-ray amorphous material. The main variability appears to be in the degree of crystallinity of the clay-size material. In general, portions of cycles highest in $CaCO_3$ contain the poorest crystalline material, as indicated by low intensities of the 3.3Å quartz peak and the (020), (110), and (111) kaolinite peaks around 20° 2θ and high X-ray amorphous "hump" between 16° and 34° 2θ. The most-crystalline, clay-size material (greatest peak intensities, lowest amorphous "hump") occurs in portions of cycles lowest in $CaCO_3$.

Variations in total numbers of calcareous nannofossils within a standardized sample and percentage of discoasters relative to total nannofossils are plotted along with percent $CaCO_3$ in Figure 12. There is a high-positive correlation between $CaCO_3$ content and numbers of nannofossils, and a high-negative correlation between percent $CaCO_3$ and relative abundance of discoasters. Plate 1 further shows

[7]Subsequent $CaCO_3$ analyses indicate that what we initially described as marl and clay may not always contain less than 60% or 30% $CaCO_3$, respectively (Figure 7). However, the $CaCO_3$ analyses do show that the darker green layers almost always represent an increase in relative abundance of clay.

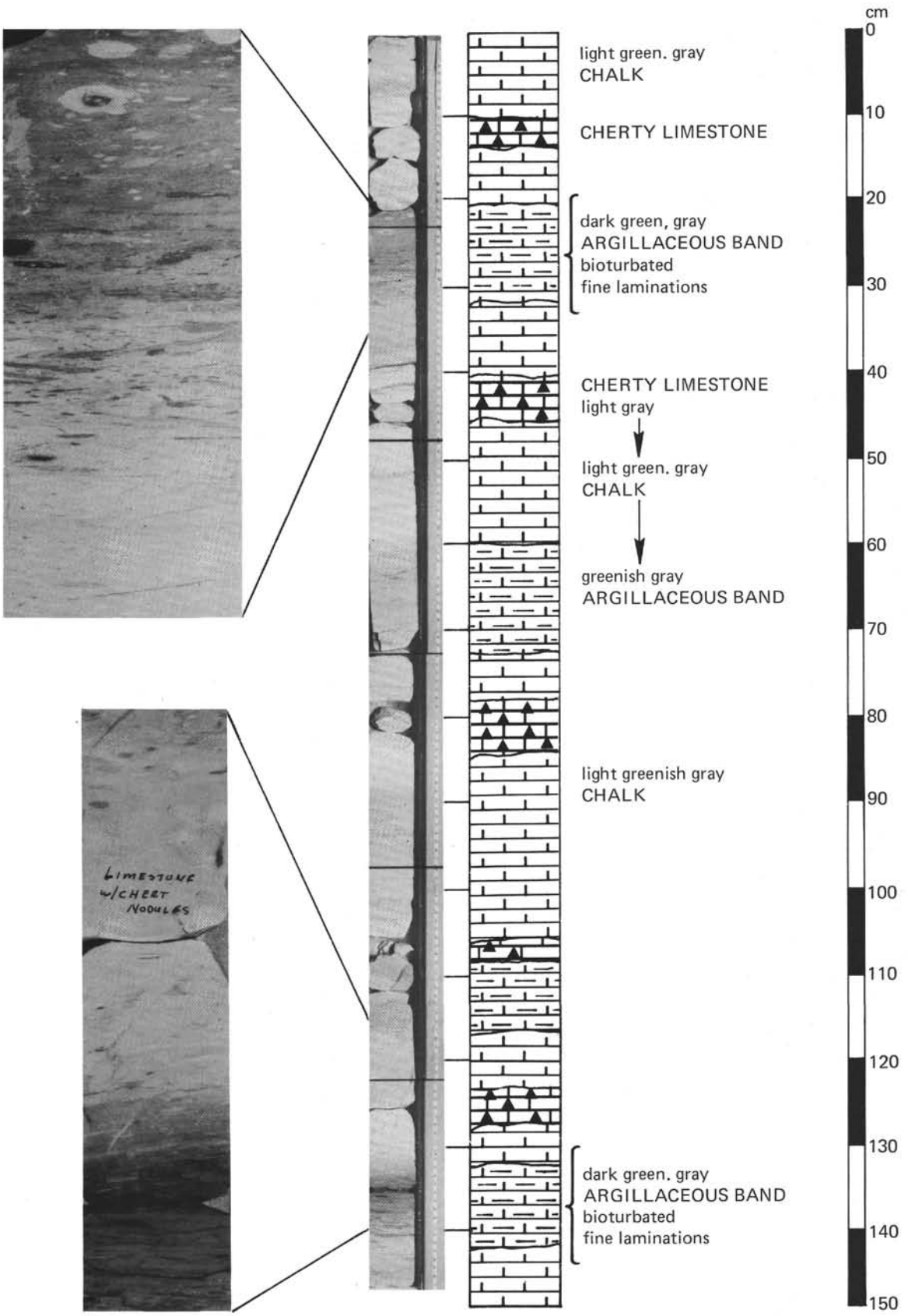

Figure 10. *Chalk-limestone-chert cycles, Site 366, Core 28, Section 5 (middle Eocene).*

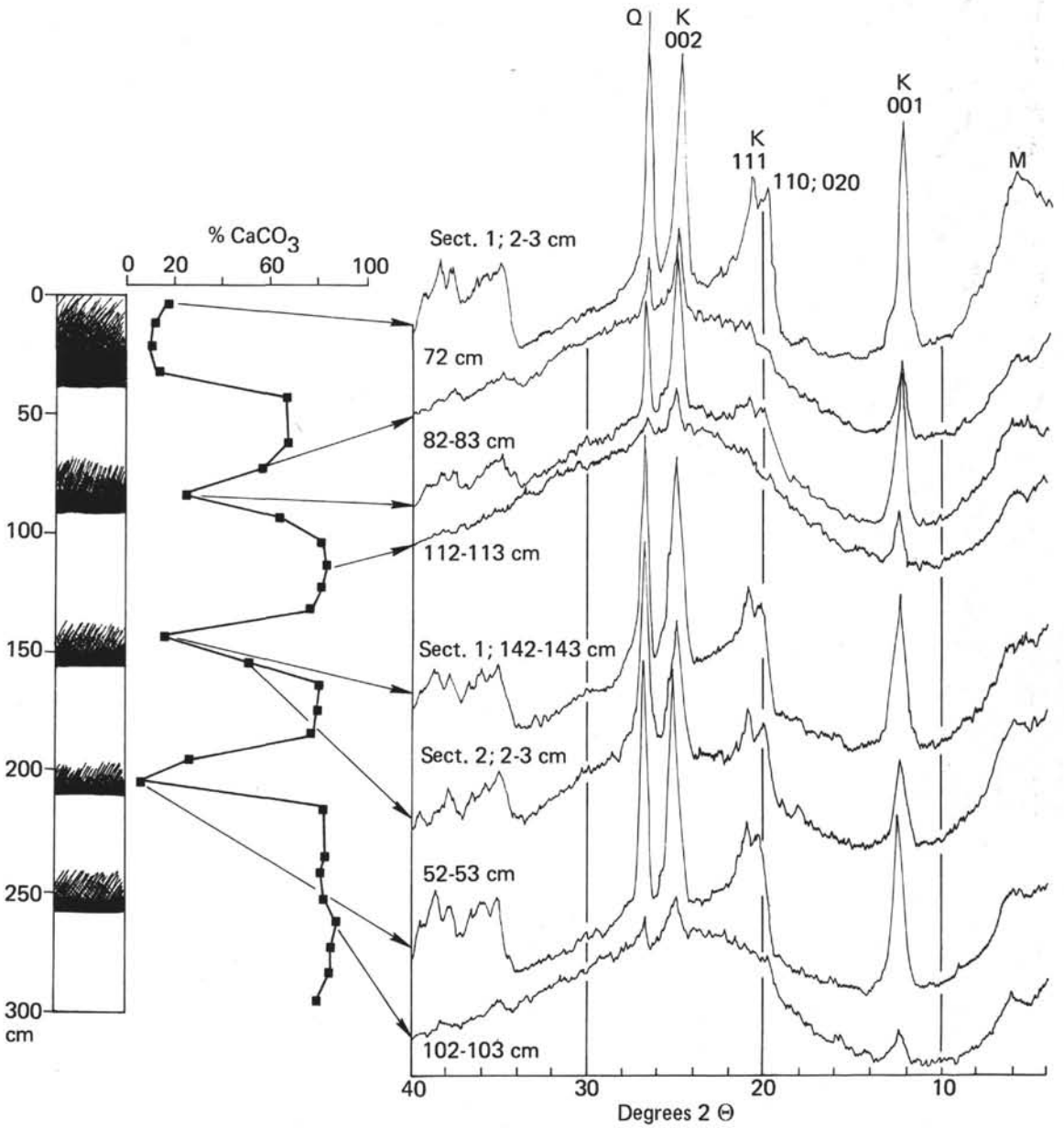

Figure 11. *Representative X-ray diffractograms from clay-rich and clay-poor portions of chalk-marl cycles, Site 366, Core 23A, Sections 1 and 2. K = kaolinite; Q = quartz; M = montmorillonite*

that coccoliths in low-carbonate portions of the cycles are more corroded than those in high-carbonate portions. Therefore, with a decrease in relative abundance of $CaCO_3$, there is marked reduction in the total nannofossil content, but nannofossils that are present are characterized by a relative decrease in abundance and degree of preservation of the more easily dissolved coccoliths and a relative increase in the more dissolution-resistant discoasters.

Coarse fractions (>63 μm and 40-63 μm) of three samples representing typical chalk, marl, and clay from well-developed chalk-marl cycles in Core 23A were analyzed by L. Diester-Haass, Kiel University (Figure 13; Table 2; see also Diester-Haass, this volume, and Sarnthein, this volume). These data show that with decreasing content of $CaCO_3$, there is a decrease in relative abundance of planktonic forams and an increase in relative abundance of Radiolaria in the sand-size fraction; those forams that are present tend to be more fragmented in marl and clay than in chalk. Also with decreasing $CaCO_3$ (increasing clastic material), there is an increase in coarse silt in the terrigenous fraction, particularly in going from marl to clay, and a decrease in the relative abundance of desert quartz (decrease in the ratio of red to white quartz grains).

Origin of the Carbonate-Clay Cycles

Cyclic variation in amount of $CaCO_3$ could be caused by fluctuations in $CaCO_3$ productivity, $CaCO_3$ dissolution, dilution by noncalcareous terrigenous material (called "clay" here), or any combination of the above. The amount of dilution or dissolution required to produce an observed percent $CaCO_3$ can be

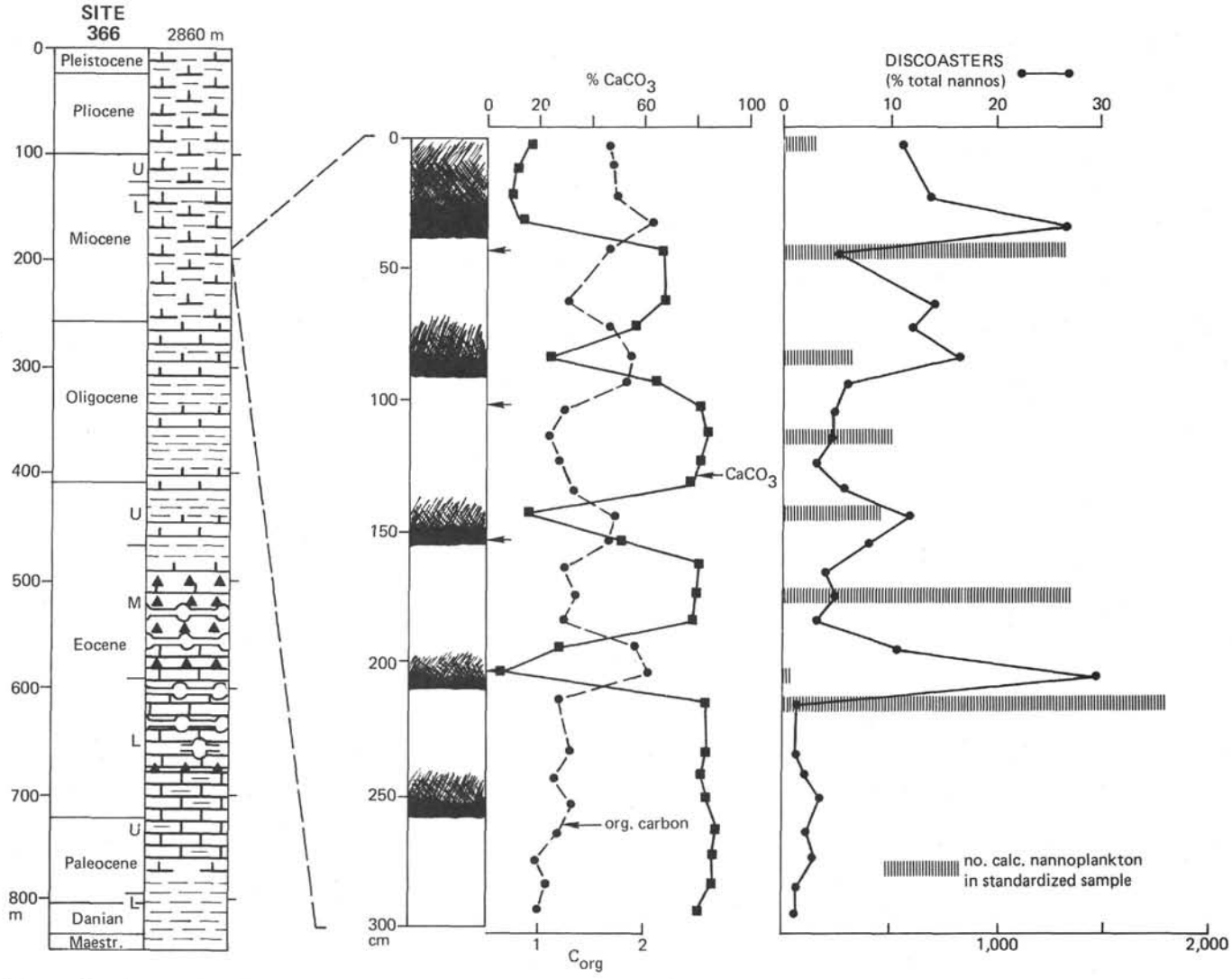

Figure 12. *Curves for % $CaCO_3$, % organic carbon, and % discoasters, and histograms of total nannofossils, Site 366, Core 23A, Sections 1 and 2. Section between 100 and 200 cm is shown in greater detail in Figure 13. Locations of samples for scanning electron micrographs in Plate 1 are indicated by arrows.*

calculated, assuming constant productivity of $CaCO_3$, using methods described by Berger (1971) and Gardner (1975). For example, the sediments of Core 23A, Sections 1 and 2 (Figure 12) have large variations in carbonate content. If we use 85% $CaCO_3$ as the pelagic carbonate baseline, then any value less than 85% $CaCO_3$ means either an addition of noncalcareous material or dissolution of the pelagic carbonate. The following equations were used:

$$L = (1\text{-}0.15/Nf)/0.0085$$
$$A = (0.85/Cf\text{-}1)/0.0015$$

where L is the percent loss of $CaCO_3$ by dissolution, A is the percent addition of noncalcareous material, Nf is the final carbonate fraction, and Cf is the observed $CaCO_3$ fraction. Curves of these two equations are shown in Figure 14. These show, for example, that to decrease the $CaCO_3$ content from 85% to 50%, either 82% of the baseline $CaCO_3$ must be dissolved or there must be an addition of 470% more clay by dilution. Using the curves in Figure 14, the $CaCO_3$ curve in Figure 12 was converted to a percent $CaCO_3$ histogram (Figure 15). Carbonate dissolution (L) and clay dilution (A) percentages were then determined for each 10-cm interval. Notice that both the A and L scales are linear, but that the L scale ranges from 0% to 100% and the A scale ranges from 0% to 9000%. In order to obtain the low-carbonate percentages observed in clay-rich portions of the cycles, a large percentage of initial $CaCO_3$ must be dissolved if only dissolution is assumed, but a tremendous increase in clay is required if we assume only dilution. For example, to get 15% $CaCO_3$ in the final product, 97% of the initial $CaCO_3$ would have to be dissolved, or the clay input would have to increase by over 3000%.

The figures of percentage loss and addition (L and A) are somewhat misleading in terms of actual volume of materials lost or added. An example is illustrated in Figure 16. To obtain a bottom-sediment column 10 cm high containing 50% clay and 50% $CaCO_3$, beginning with a sediment rain of 15% clay and 85% $CaCO_3$,

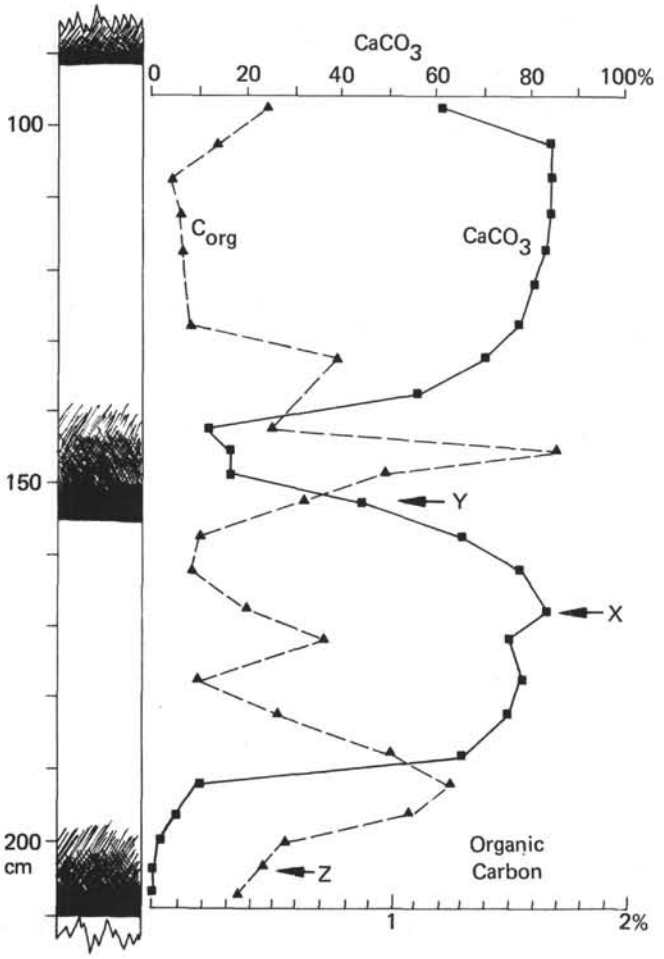

Figure 13. *Curves for % $CaCO_3$ and % organic carbon in samples collected at 5-cm intervals between 100 and 200 cm, Core 23, Sections 1 and 2, Site 366. Points marked X, Y, and Z show locations of samples for coarse-grain analyses tabulated in Table 2 (Analyses by F. C. Kogler, Kiel University).*

either 82% of the $CaCO_3$ must be dissolved or 468% more clay must be added. In terms of actual volumes of materials, this means that to get the final 10 cm, 23.3 cm of $CaCO_3$ was removed or 4.2 cm of clay was added. Thus, the dissolution process involves a much greater absolute volume change, whereas the dilution process involves a much greater relative volume change. We feel that it is this relative (percentage) change that is most important when considering the processes involved in dissolution and dilution.

The zone having the greatest rate of change of carbonate dissolution in the oceans is used to define the lysocline (Berger, 1968, 1970). The top of the calcite lysocline (often referred to loosely as *the* lysocline), particularly in the Atlantic, is related to the top of the Antarctic Bottom Water (AABW) mass (e.g., Berger, 1970), and the sharpness of the lysocline is a function of strength of bottom-water supply. Changes in rate of dissolution of $CaCO_3$ could be caused by at least two independent factors. The first is a change in the position of the lysocline relative to the sea floor. This has been suggested by many authors (Hsü and Andrews, 1970; Hay, 1970; Berger and von Rad, 1972; Luz and Shackleton, 1975; Ramsay, 1974; Gardner, 1975; Diester-Haass, 1975; among others). The second factor, postdepositional dissolution of $CaCO_3$, was discussed above.

Dilution by noncalcareous material can be accomplished by windborne material, by a nepheloid layer within the bottom water, or by river-derived material injected into the water column at several different depths. Several workers have favored dilution of Pleistocene carbonate sediments in the low-latitude Atlantic by windborne terrigenous material (Folger et al., 1967; Delany et al., 1967; Folger, 1970; Ruddiman, 1971; Carlson and Prospero, 1972; Hays and Perruzza, 1972). They all suggest that the Harmatton Winds at 5° to 20° north latitude are the transporting agents. This suggestion implies that the strength of the Harmatton Winds varies in phase with climatic episodes, a conclusion supported by the data of Gardner and Hays (1976).

Data on the quantitative load carried by a nepheloid are not generally known. However, Eittreim et al. (1975) suggest a flux of 100 μg/l. Nepheloid layers do exist along the west African continental margin, but Site 366 is above and west of any reported layers. Presumably, any increase in terrestrial runoff would increase the density of the nepheloid layer. Consequently, we can envision a fluctuating nepheloid layer keeping in phase with climatic events. These two dynamic processes, windborne and nepheloid transport, would both increase in load during more vigorous glacial periods; together they pose a potential for dilution by addition of noncalcareous material.

Extending the above information gained from analyses of Pleistocene cores to the Eocene to Miocene cycles on the Sierra Leone Rise, it would appear that both noncarbonate dilution and dissolution of $CaCO_3$ could have contributed to the $CaCO_3$-clay cycles at this site. If dilution were the dominant cause of clay variability, we reason that there might be a difference in the mineralogy of clay reaching the Sierra Leone Rise during periods of rapid dilution from that found during periods of slower dilution, regardless of whether the clay was wind- or water-transported. A difference in clay mineralogy would strongly support dilution; no difference between high- and low-clay portions of the cycles would tend to support dissolution, but it would certainly not rule out dilution.

Figure 11 shows that clay mineralogy is essentially the same in both high- and low-carbonate portions of the cycles. The dominant minerals in both portions are quartz and kaolinite with a relatively large amount of X-ray amorphous material. This assemblage simply indicates a tropical continental source for most of the noncarbonate material. The abundance of kaolinite in the clay-size fraction of sediments along the tropical coast of Africa is well documented (e.g., Biscaye, 1965; Delany et al., 1967; Griffin et al., 1968; and Lange, 1975).

Although there are no apparent changes in gross clay mineralogy between high- and low-clay portions of the cycles, there is a difference in degree of crystallinity. In general, the clays in higher clay portions of the cycles

TABLE 2
Analyses of Three Samples of Coarse-Grained Material from Chalk, Marl, and Clay, Site 366, Core 23A, Section 2[a]

	Sample X (Chalk)	Sample Y (Marl)	Sample Z (Clay)
Sample interval within section (cm)	157-158	152-153	204-205
Sand Fraction (>63μm) - % of total sediment	14.8	6.7	0.8
Coarse silt fraction (40-63μm) - % of total sediment	3.4	1.6	0.2
Planktonic foraminifera fragments - % of whole-tests + fragments	48.9	61.9	55.0
Benthonic foraminifera - % of benthonic + planktonic forams	0.66	2.1	2.1
% of sand fraction of:			
Radiolaria	6.9	14.2	63.8
Benthonic foraminifera	0.6	1.8	0.6
Planktonic foraminifera	91.3	82.7	28.0
Sponges	0.5	0.7	1.1
Ostracodes	0.1	0.1	–
Echinoderms	–	0.1	–
Fish debris	0.4	0.5	1.0
Pyrite	–	–	1.2
Ratio of planktonic foraminifera to radiolaria	13.2	5.8	0.4
Radiolaria - % of total sediment	1.02	0.95	0.51
63-125μm fraction - % of terrigenous material	0.2	–	4.3
40-63μm fraction - % of terrigenous material	5.1	4.9	25.2
Desert quartz number (red quartz grains/white quartz grains × 100)	194	147	85
$CaCO_3$ - % dry weight of sample	78.0	44.8	0.67
Organic carbon - % dry weight	0.19	0.65	0.46

[a]Analyses by L. Diester-Haass, Kiel University. See Figure 13 for location of samples.

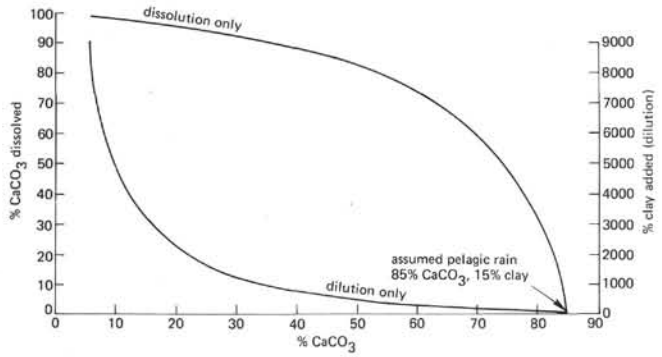

Figure 14. *Curves for % initial $CaCO_3$ dissolved and % initial clay added to obtain observed % $CaCO_3$ (0-100%) assuming dissolution only and dilution only of an initial pelagic rain of 85% $CaCO_3$, 15% clay (see text for equations for curves).*

have a higher degree of crystallinity than do the clays in high $CaCO_3$ portions. It is not clear how this variability in degree of crystallinity can be related to the problem of dilution versus dissolution, although it may have some bearing on paleoclimatic variations as discussed later.

The data on coarse fractions, presented in Table 2, show an increase in silt content only in the clay sample. If the change from chalk to marl (samples X and Y in Table 2) was the result of dilution by terrigenous material, then all of this material must have been finer than coarse silt. The data presented in Figure 15 show that a tremendous influx of terrigenous material is necessary to produce the observed variations in $CaCO_3$ and clay by dilution alone. If the material was transported by trade winds, these winds would have had to carry a great amount of clay. Presumably, most of this terrigenous material (whether wind- or water-transported) would have been derived from the Sahara, just as it is today, and yet the data in Table 2 show less desert quartz (i.e., less red quartz relative to white quartz) in the marl and clay samples than in the chalk sample.

Considering the weak mineralogical evidence, together with the magnitude of some of the $CaCO_3$ fluctuations and relative magnitudes of the dissolution and dilution processes required (Figure 15), we favor dissolution over dilution as the dominant process forming the cycles at Site 366.

Our best indicators of dissolution as the dominant cause of the $CaCO_3$ and clay cycles on the Sierra Leone

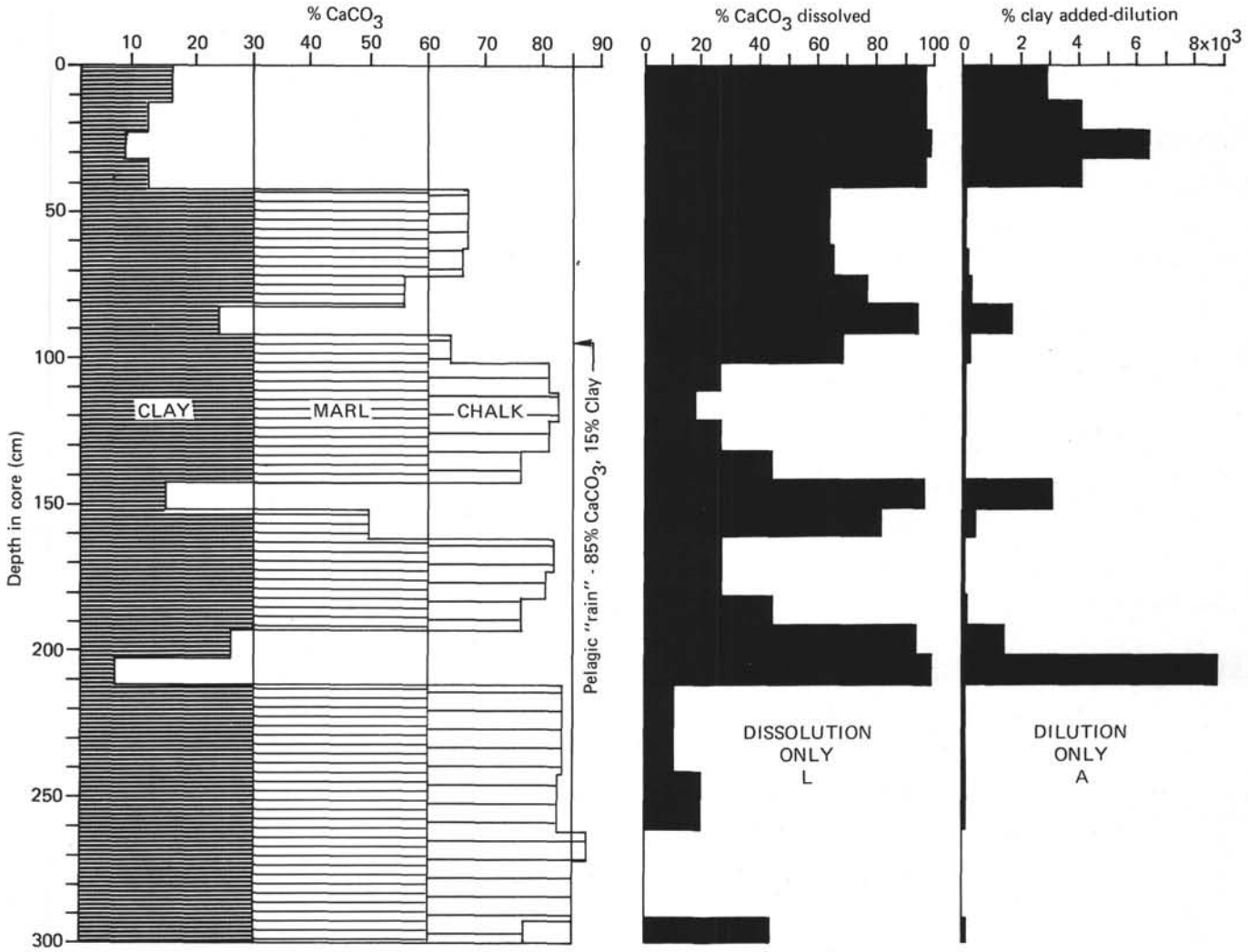

Figure 15. *Histograms of % $CaCO_3$, % initial $CaCO_3$ dissolved, and % initial clay added to obtain observed % $CaCO_3$ at Site 366, Core 23A, Sections 1 and 2, assuming dissolution only and dilution only of an initial pelagic rain of 85% $CaCO_3$, 15% clay.*

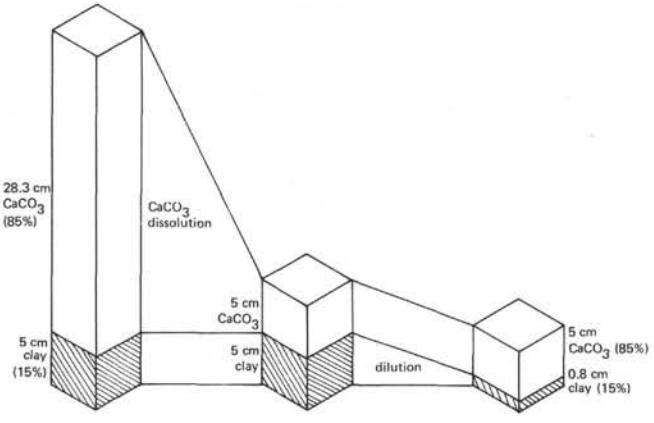

Figure 16. *Volumes of $CaCO_3$ needed to be dissolved and clay to be added, beginning with 85 % $CaCO_3$ and 15% clay and ending with 50% each of $CaCO_3$ and clay.*

Rise are the quantitative and qualitative changes in calcareous plankton. Dissolution of these organisms would be particularly sensitive to climatic changes if the top of the rise was near the lysocline at the time the sediments were accumulating. The top of the present calcite lysocline in the eastern equatorial Atlantic is approximately 4500 meters, with the CCD about 500 meters deeper. During the Miocene, the CCD, and presumably the lysocline, was as much as 1500 meters shallower (Figure 17), which would probably place the top of the Sierra Leone Rise below the lysocline and, therefore, subject to variations in dissolution of $CaCO_3$. At Site 366, there is a marked change in degree of preservation of calcareous nannofossils in the middle Miocene (Core 13A, 110 m). From middle Miocene upward, coccoliths are abundant and well preserved. However, from Paleocene through upper Miocene, coccoliths are common, but preservation is poor to moderate (Figure 18; see also Biostratigraphic Summary, Site 366 Chapter, this volume). Coccoliths suggest that Site 366 has been above the calcite lysocline only since late Miocene. Carbonate sediments accumulating on the Sierra Leone Rise prior to late Miocene time may have recorded fluctuations in the position of the lysocline.

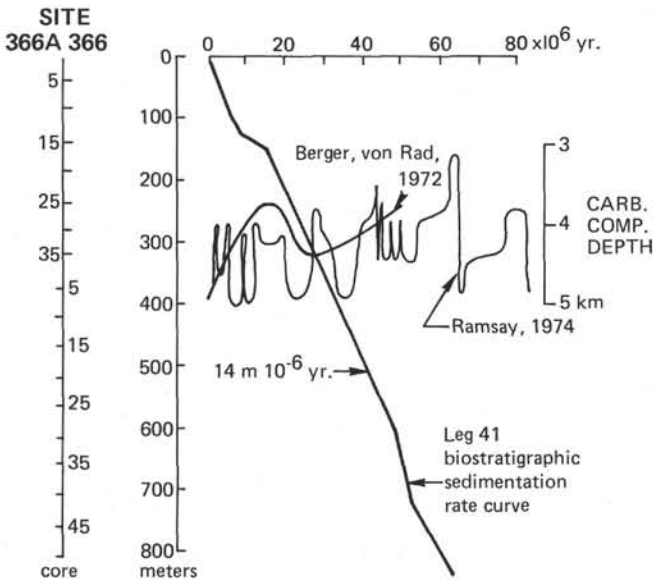

Figure 17. *Estimates of temporal variations in the calcite compensation depth (CCD) superimposed on the biostratigraphic accumulation rate curve for Site 366 (CCD estimates from Berger and van Rad, 1972; Ramsay, 1974).*

Figure 12 and Plate 1 show that the absolute number of nannoplankton individuals is markedly reduced in zones of low $CaCO_3$ in the Miocene cycles of $CaCO_3$ and clay. What is perhaps even more significant is the variation in abundance of discoasters, which are more resistant to dissolution than coccoliths (Figure 12). Discoasters constitute less than 5% of the total nannoplankton flora in high $CaCO_3$ portions of the cycles. However, with decreasing $CaCO_3$ content, relative abundance of discoasters increases to as much as 30% in low-$CaCO_3$ portions of the cycles. The same pattern appears to hold true in the more siliceous cycles of Eocene age at Site 366. For example, in the cycles of green chalk and cherty chalk of middle Eocene age, nannos are abundant and well preserved, with coccoliths much more abundant than discoasters in higher $CaCO_3$ (about 90% $CaCO_3$), cherty portions of the cycles. In the higher clay, green chalk portions of the cycles (about 80% $CaCO_3$), nannos are rare and the more resistant discoasters are in greater abundance than coccoliths, which are fragmented and corroded.

If the low $CaCO_3$ portions of the cycles were due to dilution by terrigenous material, then we would expect to find parallel fluctuations in relative abundances of $CaCO_3$, coccoliths, and discoasters. Exact opposite fluctuations in relative abundances of coccoliths and discoasters cannot be explained by dilution. The observed variations can only be explained by one process or a combination of two processes: (1) opposite variation in productivity of coccoliths and discoasters, and (2) dissolution of $CaCO_3$ resulting in a reduction in total $CaCO_3$ and relative abundance of coccoliths, and a relative increase in dissolution-resistant discoasters. It is highly unlikely that differential productivity (process 1) could produce exact-opposite fluctuations in abundance of coccoliths and discoasters, because both organisms respond similarly to environmental changes.

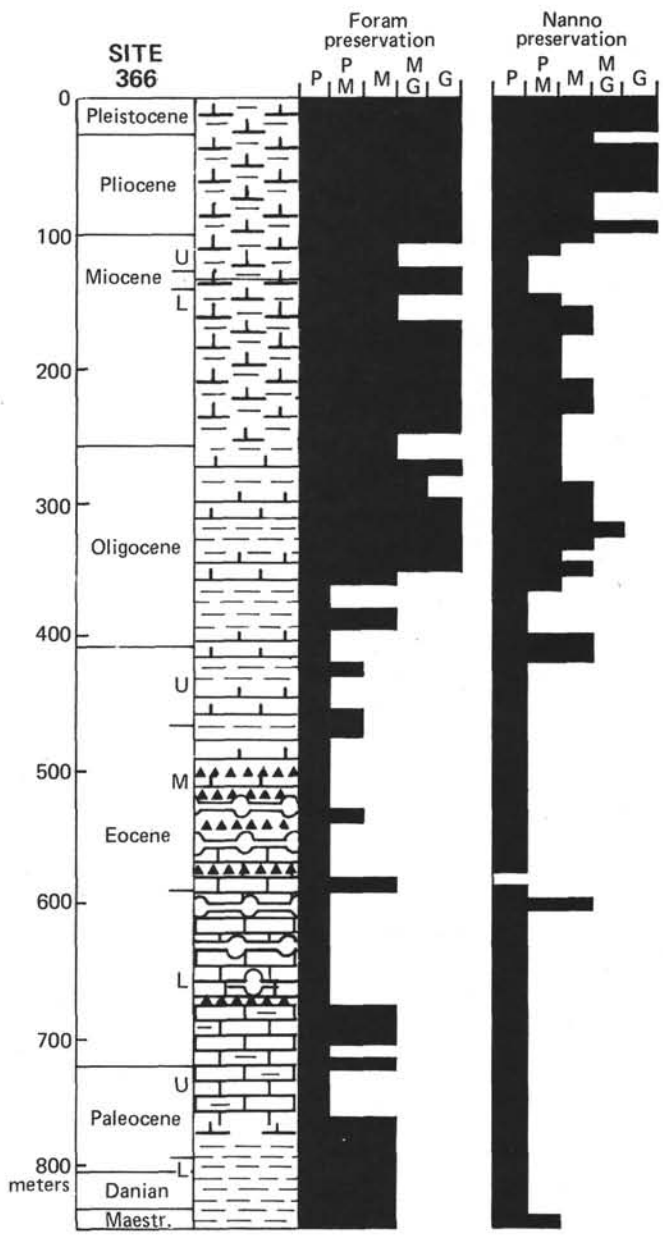

Figure 18. *Histograms of relative degree of preservation of forams and nannos, Site 366, based on shipboard estimates from core catcher samples. P = poor; M = moderate; G = good.*

This leaves dissolution of $CaCO_3$ as the only process that could have produced the observed cyclic variations in nannoplankton abundance, and as the most probable process responsible for the observed cyclic variations in $CaCO_3$ and clay. Cyclic fluctuations in rate of supply of terrigenous material may well have occurred, and to the extent that these fluctuations were in phase with cyclic fluctuations in $CaCO_3$ dissolution, the two processes could have enhanced differences in relative abundances of $CaCO_3$ and clay. Some recent investigations have shown that nannoplankton are transported to the sea floor much more rapidly than previously suspected, mainly by incorporation into zooplankton fecal pellets (e.g., Honjo, 1975; Roth et

al., 1975). This means that most dissolution of $CaCO_3$ occurs on the sea floor and not in the water column. Regardless of where dissolution occurs, the result would be the same: decrease in total numbers of nannos and relative enrichment in discoasters.

The analyses of coarse-grained biotic components presented in Table 2 also support dissolution. The abundance of planktonic foraminifera in the sand-size fraction decreases markedly in going from chalk to marl to clay, and there is a slight tendency toward increased fragmentation. Both of these trends (decrease in abundance and increase in fragmentation) are what one would expect with increasing dissolution of $CaCO_3$. With decreasing $CaCO_3$ content of the sediment, there is a marked increase in abundance of Radiolaria in the sand-size fraction and slight increases in sponge spicules and fish debris — all of which would be concentrated along with clay in the insoluble residue resulting from dissolution of $CaCO_3$. These data, particularly when considered along with the marked changes in nannoplankton composition, favor dissolution as the dominant process responsible for the cycles of $CaCO_3$ and clay on the Sierra Leone Rise.

If dissolution of $CaCO_3$ was an active process in formation of the Eocene to Miocene cycles of $CaCO_3$ and clay at Site 366, as our data suggest, the problem of the cause of dissolution still remains. Again we will borrow from Pleistocene dissolution cycle analogs, under the assumption that climatic variations that resulted in Pleistocene glacial-interglacial cycles were present at least through the rest of the Neogene and probably into the Paleogene.

During the earlier Neogene, the CCD, and presumably the lysocline, was much shallower than at present (Figure 17), so that any climatically induced fluctuations in activity of AABW would result in fluctuations in rate of dissolution at shallower depths than at present. We therefore feel that the combined effects of shoaling of the CCD (and lysocline) during the early Neogene, and climatically induced fluctuations in the position of the top of the AABW (and therefore the position of the lysocline) are the main reasons for the $CaCO_3$-clay cycles observed at Site 366 on the Sierra Leone Rise. Dilution by detrital input cannot be ruled out and may have combined with dissolution to enhance the $CaCO_3$-clay cycles, as suggested for the Pleistocene $CaCO_3$-clay cycles in the same region (Gardner, 1975).

Periodicity of the $CaCO_3$-Clay Cycles

The periodicities of the cycles described above also support the Pleistocene analog of climatically induced dissolution episodes. The redox and dissolution cycles have periods of between 30,000 and 50,000 yr, with an average around 45,000 yr. The siliceous Eocene cycles have periods ranging from 7000 to 21,000 yr. Studies of Pleistocene sediment cycles have revealed periods of cold pulses ranging from 30,000 to 150,000 yr (Ruddiman, 1971; Gardner, 1975) with the predominant periods being between 40,000 and 60,000 yr. The sediments cored on Leg 41 show this same pervasive periodicity, suggesting that climatic cycles responsible for variations in flow of AABW during the Pleistocene, and consequently for variations in the position of the lysocline, were also present in the Miocene and perhaps as far back as the Eocene.

Periodicities of cycles in sediments on the order of tens of thousands of years are common. Sediment types range from Pleistocene deep-sea sediments, to Eocene and Triassic lacustrine sediments (Bradley, 1929; Van Houten, 1964; Anderson, 1964), Miocene cherts (Bramlette, 1946; Anderson, 1964), Cretaceous limestone and chalk (Gilbert, 1895; Winkler, 1926), Pennsylvanian limestone (Anderson, 1964), and Permian evaporites (Anderson et al., 1972).

Climatic changes related to the earth's precession cycle of about 23,000 yr have been suggested (e.g., Milankovitch, 1930; Anderson, 1964; Broecker and van Donk, 1970; Matthews, 1974; Hays et al., 1976). Milankovitch (1930) further suggested that the earth's orbital cycles of precession, obliquity, and eccentricity (periods of about 23,000 yr, 41,000 yr, and 100,000 yr, respectively) are the main driving mechanisms behind long-term climatic change. Matthews (1974) refers to these cycles as the "tuning forks" for geologic time, and Hays et al. (1976) go so far as to state that the sedimentary records of these cycles provide more accurate dating than present radiometric dating techniques, at least for the past 400,000 yr. We suggest that this record probably goes back much farther.

Tertiary Climates of Northwest Africa

We can go one step further in the application of our uniformitarian analog that the Pleistocene is the key to the Miocene and maybe the Eocene, and speculate on the continental climatic regime of northwest Africa. If the pre-Pleistocene carbonate cycles are a response to cold-warm pulses as they apparently are in the Pleistocene, then we might expect continental climates to vary in much the same way as they did during the Pleistocene. During the cold periods of the Pleistocene, northwest Africa in general was colder and dryer than during warm periods (Gates, 1976). Diester-Haass et al. (1973) and Diester-Haass (1976) suggest that during glacial periods the Mediterranean climatic belt shifted south as far as 20°N. Under these conditions, we might expect to have an increase in rate of wind erosion associated with southern expansion of the Sahara, as indicated in Michel (1973), too. This would be particularly true if the intensity of equatorial trade winds increased, as suggested by Ruddiman (1971), Hays and Perruzza (1972), Parkin and Shackleton (1973), Sarnthein and Walger (1974), Gardner and Hays (1976), and Diester-Haass (1976). Indeed, Gates' (1976) model for ice-age atmospheric conditions predicts that present wind patterns would be shifted to lower latitudes and increased somewhat in strength during glacial periods. Increased wind erosion would tend to enhance differences in clay and $CaCO_3$ brought about by dissolution. Under cold/dry conditions, we would also expect less-intense chemical weathering due to lower temperature and decreased available moisture. Although the interrelationships are extremely complex, decreased decomposition of soil materials would

explain the observed increase in clay crystallinity during carbonate lows, presumed to correspond to climatic cold periods (Figure 11). With increases in temperature and available moisture, soil materials would experience greater decomposition, with a resultant decrease in crystalline material and an increase in X-ray amorphous clay.

SUMMARY AND CONCLUSIONS

The most common cyclic sediments cored on Leg 41 are turbidites. They are particularly common in the Paleocene, Eocene, and Miocene sections at Site 368, throughout the entire section at Site 370 (Lower Cretaceous to Holocene), and in the Cretaceous section at Site 367. The turbidites have periods on the order of 10,000 yr.

Most redox cycles observed are manifested as color changes and appear to be related to cyclic variations in the amount of organic matter in the sediments. Cycles of green and black clay or shale appear to be the result of pulsing terrigenous input, including organic material, from the African continent. A similar interpretation, with less organic matter involved, applies to cycles of red and green clay or shale observed at several sites. Pulsing organic material probably also produced striking cycles of white limestone and black marlstone of Late Jurassic to Early Cretaceous age in the Cape Verde Basin, which are the lithologic equivalents of organic-rich marls cored in the North American Basin on DSDP Leg 11, and the "Marne a Fucoide" facies of the Tethyan Mediterranean. All of these organic-rich, organic-poor cycles have periods on the order of 50,000 yr; they are interpreted as having resulted from a climatically induced cyclic influx of organic matter that caused cyclic variations in reducing conditions within the sediments and, at times, for some distance above the sediment-water interface. The sedimentary record at Site 367 indicates that pulsing of organic material began in Late Jurassic and continued at least through Eocene.

Another example of cyclic redox fluctuations is illustrated by the striking red and light-green nodular limestones of Late Jurassic age, cored at Site 367; these are correlated with Late Jurassic nodular limestones in the North American Basin cored on Leg 11, and with the classic Jurassic Tethyan section (Ammonitico Rosso) of the Mediterranean. The red and light green colorations may have resulted from fluctuating redox conditions in the sediments related to organic matter, or they may represent cyclic fluctuations in solution-reprecipitation of $CaCO_3$.

Silica diagenesis is common in Leg 41 sediments, sometimes related to other cycles and sometimes forming separate cycles. Silica diagenesis is apparently related to primary porosity within sediments and, hence, the silica cycles generally exhibit a systematic relationship with other cycles, such as chert development in coarser portions of turbidite-graded bedding.

Carbonate-clay cycles in the lower Pliocene to lower Miocene section at Site 368 on the Cape Verde Rise are interpreted as having resulted mainly from pulsing of supply of terrigenous material, superimposed on increasing preservation of pelagic $CaCO_3$ as the site was uplifted above the calcite compensation depth beginning in middle Miocene. Dissolution undoubtedly also contributed to variations in percentages of clay and $CaCO_3$, but probably became less important as the site was elevated and the lysocline lowered.

Cycles of $CaCO_3$ and clay in the Eocene to middle Miocene portions of the Sierra Leone Rise section are interpreted as resulting from cyclic variations in dissolution of $CaCO_3$, possibly aided by influx of terrigenous material. These cycles are similar to the largely dilution $CaCO_3$-clay cycles at Site 368 and indicate that clay enrichment by either dissolution or dilution can result in similar products.

The upper Eocene to middle Miocene chalk-marl cycles have periods ranging from 29,000 to 50,000 yr. The Eocene siliceous cycles have periods ranging from 7000 to 21,000 yr. The periods of these cycles, as well as the climatically induced organic-rich/organic-poor cycles at Sites 367 and 368, are similar to periods of Pleistocene climatic cycles. This would suggest that cycles of the earth's movement, believed to be the causes of long-term climatic change in the Pleistocene, extended back into at least the Tertiary.

The carbonate-clay cycles observed at Site 366 on the Sierra Leone Rise may be equivalent to dissolution cycles of the same approximate age observed on DSDP Leg 40 at Site 362 on the Walvis Ridge (Bolli, Ryan, et al., 1975), and on Leg 39 at Site 354 on the Ceara Rise (Perch-Nielsen, Supko, et al., 1975). On the Ceara Rise, cyclic sediments are interpreted to be the result of variations in the rate of sediment accumulation, although fluctuations in CCD or corrosive bottom waters were also suggested as possibilities. Although Site 362 on the Walvis Ridge is shallow (1325 m), distinct periods of dissolution were noted in the Oligocene, middle Miocene, and Eocene portions of the section. Dissolution is interpreted as having resulted from fluctuating CCD, which, in turn, resulted from pulsing Antarctic Bottom Water (AABW). Dissolution cycles were also found on Leg 40 in the Miocene, Oligocene, and Eocene sections at Sites 360 (water depth of 2949 m) and 364 (water depth of 2448 m).

In Figure 19 we have interpreted mid-Tertiary sedimentation on the Sierra Leone Rise in terms of fluctuations in Antarctic Bottom Water, position of the lysocline, rate of dissolution of $CaCO_3$, and rate of dilution by terrigenous material. These systems are inferred from the cyclic variations in $CaCO_3$ and clay, clay mineralogy, and nannofossil abundance and preservation. Conditions on North Africa are interpreted in terms of temperature, available moisture, rates of weathering and erosion, and trade-wind intensity.

ACKNOWLEDGMENTS

We would like to thank Dr. Douglas W. Kirkland, Mobil Research and Development Corporation, Dallas, Texas, for critically reviewing this paper and L. Diester-Haass of University of Kiel, Kiel, Germany for the three analyses in Table 2.

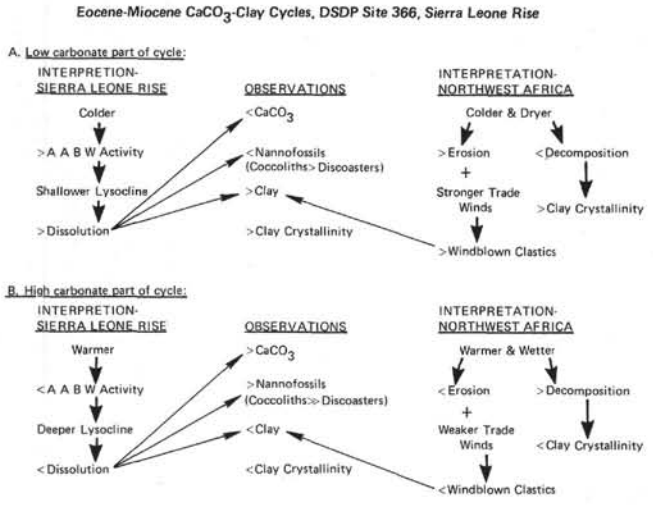

Figure 19. *Summary of observations and interpretations for the lower Eocene to middle Miocene carbonate-clay cycles on the Sierra Leone Rise (Site 366).*

REFERENCES

Anderson, R.Y., 1964. Varve calibration of stratification: Kansas Geol. Survey Bull. 169, p. 1-20.

Anderson, R.Y., Dean, W.E., Kirkland, D.W., and Snider, H.I., 1972. Permian Castile varved evaporite sequence, west Texas and New Mexico: Geol. Soc. Am. Bull., v. 83, p. 59-86.

Berger, W.H., 1968. Planktonic foraminifera: selective solution and paleoclimatic interpretation: Deep-Sea Res., v. 15, p. 31-43.

———, 1970. Planktonic foraminifera: selective solution and the lysocline: Marine Geol., v. 8, p. 111-138.

———, 1971. Sedimentation of planktonic foraminifera: Marine Geol., v. 11, p. 325-358.

Berger, W.H. and von Rad, U., 1972. Cretaceous and Cenozoic sediments from the Atlantic Ocean. *In* Hays, D.E., Pimm, A.C., et al., Initial Reports of the Deep Sea Drilling Project, Volume 14: Washington (U.S. Government Printing Office), p. 787-918.

Bernoulli, D., 1972. North Atlantic and Mediterranean Mesozoic facies: A comparison. *In* Hollister, C.D., Ewing, J.I., et al., Initial Reports of the Deep Sea Drilling Project, Volume 11: Washington (U.S. Government Printing Office), p. 801-871.

Bernoulli, D. and Jenkyns, H.C., 1974. Alpine, Mediterranean, and central Atlantic Mesozoic facies in relation to the early evolution of the Tethys. *In* Dott, R.H., Jr.and Shaver, R.H. (Eds.), Modern and ancient geosynclinal sedimentation: Soc. Econ. Paleontol. Mineralog. Spec. Publ. 19, p. 129-160.

Biscaye, P.E., 1965. Mineralogy and sedimentation of Recent deep-sea clay in the Atlantic Ocean and adjacent seas and oceans: Geol. Soc. Am. Bull., v. 76, p. 803-832.

Bolli, H.M., Ryan, W.B.F., McKnight, B.K., Kagami, H., Melguen, M., Siesser, W.G., Natland, J., Longoria, J.F., Proto-Decima, F., Foresman, J.B., and Hottman, W.E., 1975. Basins and margins of the eastern South Atlantic: Geotimes, v. 20, p. 22-24.

Bosellini, A. and Winterer, E.L., 1975. Pelagic limestone and radiolarite of the Tethyan Mesozoic: A genetic model: Geology, v. 3, p. 279-282.

Bradley, W.H., 1929. The varves and climate of the Green River epoch: U.S. Geol. Surv. Prof. Paper 158, p. 87-110.

Bramlette, M.N., 1946. The Monterey Formation of California and the origin of its siliceous rocks: U.S. Geol. Surv. Prof. Paper 212, p. 1-57.

Broecker, W.S., 1971. Calcite accumulation rates and glacial to interglacial changes in oceanic mixing. *In* Turekian, K.K. (Ed.), The Late Cenozoic glacial ages: New Haven (Yale Univ. Press), p. 239-265.

Broecker, W.S. and van Donk, J., 1970. Insolation changes, ice volumes, and the 0^{18} record in deep-sea cores: Rev. Geophys., v. 8, p. 169-198.

Carlson, T.N. and Prospero, J.M., 1972. The large-scale movement of Saharan air outbreaks over the northern equatorial Atlantic: J. Appl. Meterol., v. 11, p. 283-297.

Delany, A.C., Parkin, D.W., Griffin, J.J., Goldberg, E.D., and Reinmann, B.E.F., 1967. Airborn dust collected at Barbados: Geochim. Cosmochim. Acta, v. 31, p. 885-909.

Diester-Haass, L., 1975. Sedimentation and climate in the late Quaternary between Senegal and the Cape Verde Islands: Meteor Forsch. Ergebn., v. 20, p. 1-32.

———, 1976. Late Quaternary climatic variations in NW Africa deduced from East Atlantic sediment cores: Quat. Res., v. 6.

Diester-Haass, L., Schrader, H.-J., and Thiede, J., 1973. Sedimentological and paleoclimatological investigations of two pelagic ooze cores off Cape Barbas, North-West Africa: Meteor Forsch. Ergebn, v. 16, p. 19-66.

Ettreim, S., Biscaye, P.E., and Amos, A.F., 1975. Benthic nepheloid layers and the Ekman thermal pump: Geol. Soc. Am. Abstract with Programs, v. 7, p. 1066-1067.

Folger, D.W., 1970. Wind transport of land-derived mineral, biogenic, industrial matter over the North Atlantic: Deep-Sea Res., v. 17, p. 337-352.

Folger, D.W., Burckle, L.H., and Heezen, B.C., 1967. Opal phytoliths in a North Atlantic dust fall: Science, v. 155, p. 1243-1244.

Gardner, J.V., 1975. Late Pleistocene carbonate dissolution cycles in the eastern equatorial Atlantic. *In* Sliter, W.V., Bé, A.W.H., and Berger, W.H. (Eds.), Dissolution of deep-sea carbonates: Cushman Found. Foram. Res., Spec. Publ. 13, p. 129-141.

Gardner, J.V. and Hays, J.D., 1976. The eastern equatorial Atlantic: sea-surface temperature and circulation responses to global climatic change during the past 200,000 years. *In* Cline, R.M. and Hays, J.D. (Eds.), Investigations of late Quaternary paleooceanography and paleoclimatology: Geol. Soc. Am. Mem. 145.

Gates, W.L., 1976. Modeling the ice-age climate: Science, v. 191, p. 1138-1144.

Gilbert, G.K., 1895. Sedimentary measurement of Cretaceous time: J. Geol., v. 3, p. 121-127.

Griffin, J.J., Windom, H., and Goldberg, E.D., 1968. The distribution of clay minerals in the World Ocean: Deep-Sea Res., v. 15, p. 433-459.

Hay, W.W., 1970. Sedimentation rates; calcium carbonate compensation. *In* Bader, R.G., et al., Initial Reports of the Deep Sea Drilling Project, Volume 4: Washington (U.S. Government Printing Office), p. 455-540.

Hays, D.E., Imbrie, J., and Shackleton, N.J., 1976. The pacemaker of long term climatic change (abs.): Am. Geophys. Union Trans., v. 57, p. 259.

Hays, J.D. and Perruzza, A., 1972. The significance of calcium carbonate oscillations in eastern equatorial Atlantic deep-sea sediments for the end of the Holocene warm interval: Quat. Res., v. 2, p. 355-363.

Hays, J.D., Pimm, A.C., et al., 1972. Initial Reports of the Deep Sea Drilling Project, Volume 14: Washington (U.S. Government Printing Office).

Hollister, E.D., Ewing, J.I., et al., 1972. Initial Reports of the Deep Sea Drilling Project, Volume 11: Washington (U.S. Government Printing Office).

Honjo, S., 1975. Dissolution of suspended coccoliths in the deep-sea water column and sedimentation of coccolith ooze. *In* Sliter, W.V., Bé, A.W.H., and Berger, W.H. (Eds.), Dissolution of deep-sea carbonates: Cushman Found. Foram. Res. Spec. Publ. 13, p. 114-127.

Hsü, K.J. and Andrews, J.E., 1970. Lithology. *In* Maxwell, A.E., et al., Initial Reports of the Deep Sea Drilling Project, Volume 3: Washington (U.S. Government Printing Office), p. 445-453.

Jenkyns, H.C., 1974. Origin of red nodular limestones (Ammonitico Rosso, Knollenkalke) in the Mediterranean Jurassic: a diagenetic model. *In* Hsü, K.J. and Jenkyns, H.C. (Eds.), Pelagic sediments: on land and under the sea: Internatl. Assoc. Sedimentol., Spec. Publ. 1, p. 249-271.

Lange, H., 1975. Herkunft und Verteilung von Oberflächensedimenten des westafrikanischen Schelfs und Kontinental-hanges: Meteor Forsch. Ergebn., v. 22, p. 61-84.

Luz, B. and Shackleton, N.J., 1975. $CaCO_3$ solution in the tropical east Pacific during the past 130,000 years. *In* Sliter, W.V., Bé, A.W.H., and Berger, W.H. (Eds.), Dissolution of deep-sea carbonates: Cushman Found. Foram. Res., Spec. Publ. 13, p. 142-150.

Matthews, R.K., 1974. Dynamic stratigraphy: Englewood Cliffs (Prentice-Hall, Inc.).

Michel, P., 1973. Les bassins des fleuves Sénégal et Gambie: Etude géomorphologique: Mém. ORSTOM, No. 63, Paris, 752 p.

Milankovitch, M., 1930. Mathematische Klimalehre und Astronomische Theorie der Klimaschwankungen. *In* Koppen, W. and Geiger, R. (Eds.), Handbuch der Klimatologie, v. 1, pt. A, p. 176.

Müller, J. and Fabricius, F., 1974. Magnesian calcite nodules in the Ionian deep sea — an actualistic model for the formation of some nodular limestones. *In* Hsü, K.J. and Jenkyns, H.C. (Eds.), Pelagic sediments: on land and under the sea: Internatl. Assoc. Sedimentol., Spec. Publ. 1, p. 235-247.

Nesteroff, W.D., 1973. Petrography and mineralogy of sapropels. *In* Ryan, W.B.F., Hsü, K.J., et al., Initial Reports of the Deep Sea Drilling Project, Volume 13: Washington (U.S. Government Printing Office), p. 713-720.

Parkin, D.W. and Shackleton, N.J., 1973. Trade wind and temperature correlations down a deep-sea core off the Saharan coast: Nature, v. 245, p. 455-457.

Perch-Nielsen, K., Supko, P.R., Borsma, A., Bonatti, E. Carlson, R.L., Dinkelman, M.G., Fodor, R.V., Kumar, N., McCoy, F., Neprochnov, Y.P., Thiede, J., and Zimmerman, H.B., 1975. Leg 39 examines facies changes in South Atlantic: Geotimes, v. 20, p. 26-28.

Ramsay, A.T.S., 1974. The distribution of calcium carbonate in deep sea sediments. *In* Hay, W.W. (Ed.), Studies in paleooceanography: Soc. Econ. Paleontol. Mineral. Spec. Publ. 20, p. 58-76.

Roth, P.H., Mullin, M.M., and Berger, W.H., 1975. Coccolith sedimentation by fecal pellets: laboratory experiments and field observations: Geol. Soc. Am. Bull., v. 86, p. 1079-1084.

Ruddiman, W.F., 1971. Pleistocene sedimentation in the equatorial Atlantic: Stratigraphy and faunal paleoclimatology: Geol. Soc. Am. Bull., v. 82, p. 283-302.

Sarnthein, M. and Walger, E., 1974. Der äolische Sandstrom aus der West-Sahara zur Atlantikküste: Geol. Rundschau, v. 63, p. 1065-1087.

Van Houten, F.B., 1964. Cyclic lacustrine sedimentation, Upper Triassic Lockatong Formation, central New Jersey and adjacent Pennsylvania. *In* Merriam, D.F. (Ed.), Symposium on cyclic sedimentation: State Geol. Survey Kansas Bull. 169, p. 497-531.

Winkler, A., 1926. Zum schichtungs-problem: Neues Jahrb., Beilage, Band 53, p. 271-314.

PLATE 1

Scanning electron micrographs of samples from high carbonate (Figures 1-4) and low carbonates (Figures 5-8) portions of chalkmarl cycles, Site 366, Core 23A, Sections 1 and 2. For each pair of photographs, the photograph on the right is a general view, and the one on the left is a high magnification close-up of individual coccoliths.

Figures 1, 2 Sample 366-23A-1, 42-43 cm.

Figures 3, 4 Sample 366-23A-1, 102-103 cm.

Figures 5, 6 Sample 366-23A-2, 2-3 cm.

Figures 7, 8 Sample 366-23A-2, 52-53 cm.

PLATE 1

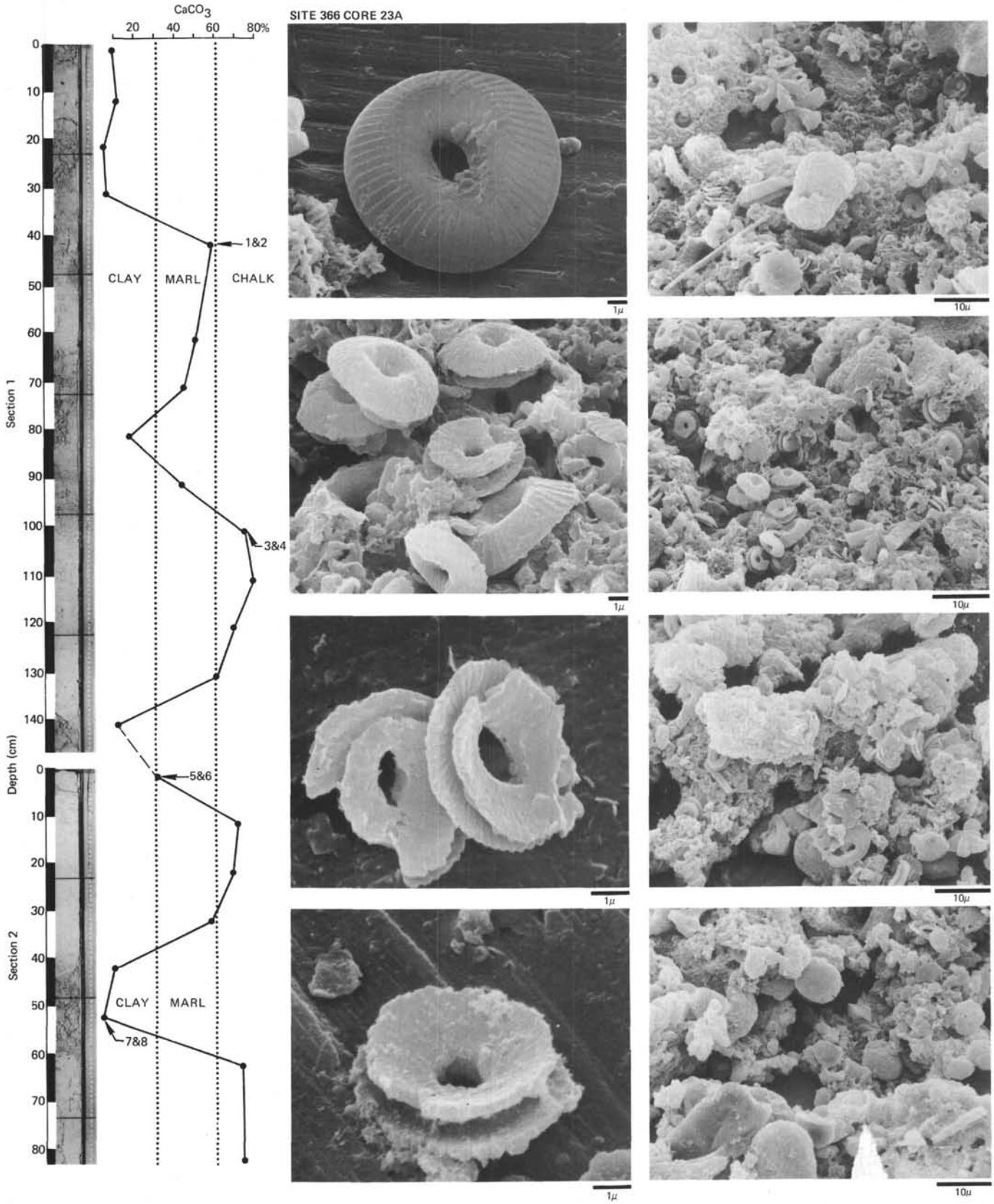
CaCO3
20
40
60
80%
SITE 366 CORE 23A
Section 1
Depth (cm)
Section 2
1&2
3&4
5&6
7&8
CLAY
MARL
CHALK
CLAY
MARL
1μ
10μ